

LA-4437-MS

CIC-14 REPORT COLLECTION  
**REPRODUCTION  
COPY**

**B. 3**

**LOS ALAMOS SCIENTIFIC LABORATORY**  
of the  
**University of California**  
LOS ALAMOS • NEW MEXICO

Quarterly Status Report on the  
**Advanced Plutonium Fuels Program**  
January 1-March 31, 1970



UNITED STATES  
ATOMIC ENERGY COMMISSION  
CONTRACT W-7405-ENG-36

## LEGAL NOTICE

This report was prepared as an account of Government sponsored work. Neither the United States, nor the Commission, nor any person acting on behalf of the Commission:

A. Makes any warranty or representation, expressed or implied, with respect to the accuracy, completeness, or usefulness of the information contained in this report, or that the use of any information, apparatus, method, or process disclosed in this report may not infringe privately owned rights; or

B. Assumes any liabilities with respect to the use of, or for damages resulting from the use of any information, apparatus, method, or process disclosed in this report.

As used in the above, "person acting on behalf of the Commission" includes any employee or contractor of the Commission, or employee of such contractor, to the extent that such employee or contractor of the Commission, or employee of such contractor prepares, disseminates, or provides access to, any information pursuant to his employment or contract with the Commission, or his employment with such contractor.

This LA . . MS report presents the status of the LASL Advanced Plutonium Fuels Program. Previous Quarterly Status Reports in this series, all unclassified, are:

LA-3607-MS	LA-3745-MS	LA-3933-MS	LA-4193-MS
LA-3650-MS	LA-3760-MS*	LA-3993-MS	LA-4284-MS
LA-3686-MS	LA-3820-MS	LA-4073-MS	LA-4307-MS
LA-3708-MS*	LA-3880-MS	LA-4114-MS	LA-4376-MS

This report, like other special-purpose documents in the LA . . MS series, has not been reviewed or verified for accuracy in the interest of prompt distribution.

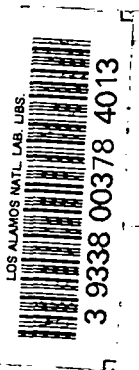
\*Advanced Reactor Technology (ART) series

Distributed. May 1970

LA-4437-MS  
SPECIAL DISTRIBUTION

**LOS ALAMOS SCIENTIFIC LABORATORY**  
of the  
**University of California**  
LOS ALAMOS • NEW MEXICO

Quarterly Status Report on the  
**Advanced Plutonium Fuels Program**  
January 1-March 31, 1970



## FOREWORD

This is the fifteenth quarterly report on the Advanced Plutonium Fuels Program at the Los Alamos Scientific Laboratory.

Studies on Fast Reactor Metallic Fuels, formerly reported as Project 461 in this series of documents, have been discontinued except for phase-out effort. Any results from the final work will be described under Project 467, a new work category covering all irradiation experiments (chiefly those concerned with (U, Pu)C fuels).

Most of the investigations discussed here are of the continuing type. Results and conclusions described may therefore be changed or augmented as the work continues. Published reference to results cited in this report should not be made without obtaining explicit permission to do so from the person in charge of the work.

## CONTENTS

<u>PROJECT</u>	<u>PAGE</u>
401 EXAMINATION OF FAST REACTOR FUELS	1
I. Introduction	1
II. Equipment Development	1
III. DP West Facility	3
IV. Methods of Analysis	4
V. Examination of Unirradiated Fuels	5
VI. Requests from DRDT	5
VII. References	6
462 SODIUM TECHNOLOGY	7
463 CERAMIC PLUTONIUM FUEL MATERIALS	8
I. Introduction	8
II. Synthesis and Fabrication	8
III. Properties	9
IV. Analytical Chemistry	20
V. References	20
464 STUDIES OF Na-BONDED (U, Pu)C LMFBR FUELS	22
465 REACTOR PHYSICS	23
I. Introduction	23
II. Cross-Section Procurement, Evaluation, and Testing	23
III. Reactor Analysis Methods and Concept Evaluations	25
References	30
467 FUEL IRRADIATION EXPERIMENTS	31
I. Introduction	31
II. EBR-II Irradiation Testing	31
III. Thermal Irradiations of Sodium Bonded Mixed Carbides	32
IV. Thermal Irradiation of Sodium Bonded U-Pu-Zr	32
501 STANDARDS, QUALITY CONTROL, AND INSPECTION OF PRODUCTS	34
I. Introduction	34
II. Phase II, LMFBR/FFTF Fuel Development Analytical Chemistry Program	34
III. Investigation of Methods	34

PROJECT 401

EXAMINATION OF FAST REACTOR FUELS

Person in Charge: R. D. Baker  
Principal Investigators: J. W. Schulte  
J. A. Leary  
C. F. Metz

I. INTRODUCTION

This project is directed toward the examination and comparison of the effects of neutron irradiation on LMFBR Program fuel materials. Unirradiated and irradiated materials will be examined as requested by the Fuels and Materials Branch of DRDT. Capabilities are established for providing conventional pre-irradiation and post-irradiation examinations. Additional capabilities include less conventional properties measurements which are needed to provide a sound basis for steady-state operation of fast reactor fuel elements, and for safety analysis under transient conditions.

Analytical chemistry methods that have been modified and mechanized for hot cell manipulators will continue to be applied to the characterization of irradiated fuels. The shielded electron microprobe and emission spectrographic facilities will be used in macro and micro examinations of various fuels and clads. In addition, new capabilities will be developed with emphasis on gamma scanning and analyses to assess spatial distribution of fuel and fission products.

High temperature properties of unirradiated LMFBR fuel materials are now being determined by Contractor in an associated project (ident no. 07463). Equipment designs and interpretive experience gained in this project are being extended to provide unique capabilities such as differential thermal analysis, melting point determination, high temperature dilatometry, and high temperature heat content and heat of fusion for use on irradiated materials.

II. EQUIPMENT DEVELOPMENT

A. Inert Atmosphere Systems  
(C. E. Frantz, P. A. Mason, R. F. Velkinburg)

During this period the high pressure argon system was installed and placed in service. Inert atmospheres were maintained in the 3 containment boxes almost exclusively by the single-pass operation.

Narrow band Photohelic controllers were incorporated into the exhaust system of all three containment boxes to provide better control over the pressure differential and thereby minimize air in-leakage.

The recirculating purification system for the disassembly cell was shown to have a capacity for absorbing up to 30 ppm O<sub>2</sub> on a continuous basis. However, since the atmosphere in this cell contained between 35 and 50 ppm O<sub>2</sub> during this Quarter, it was not possible to leave the regeneration system in continuous service. An analysis of operations has shown that transfer of materials to the boxes introduces an excessive amount of air. Efforts are being made to lower the O<sub>2</sub> concentration by the following means:

1. Improve the purging system for the transfer container.
2. Develop the technique and equipment for using a remote probe located inside the box but connected to a gas analyzer outside the box, for checking the more probable leak areas, viz., manipulator boots, and the two transfer system openings.
3. Install and test a pair of sealed manipulators

which are scheduled for arrival in October.

In the two metallography preparation cells the O<sub>2</sub> concentrations have been maintained at 1000-2500 ppm. Moisture concentrations generally were less than 40 ppm; aqueous etching solutions are used in one of the boxes. Repairs and modifications are still being made to the recirculating purification system which services the two metallography cells.

Work was started to provide the capability for a single-pass argon system for four additional containment boxes. This work necessitates minor changes in the piping and the installation of differential pressure controllers in the exhaust systems. Two cells are currently equipped for chemistry operations, and the remaining two have been provided with equipment to run differential thermal analyses and heat content measurements. It is intended that inert atmosphere be provided to these four boxes on an intermittent basis in order to supplement and extend existing capabilities.

#### B. Equipment Development

(G. R. Brewer, E. L. Ekberg, F. J. Fitzgibbon, C. E. Frantz, D. D. Jeffries, M. E. Lazarus, J. M. Ledbetter, J. L. Lehmann, C. D. Montgomery, F. H. Newbury, T. Romanik, T. J. Romero, A. E. Tafoya, J. R. Trujillo, R. F. Velkinburg, L. A. Waldschmidt)

##### 1. DTA

A change was made from a complex mirror system to a direct path through the hot cell window to provide better observation with the pyrometer. A dry run cycle was made on an empty tantalum container to establish the temperature correction to compensate for the effect of the lead glass window.

A series of calibration runs was made, and the results obtained indicated that the equipment was operational.

Two samples of irradiated (U,Pu)O<sub>2</sub> were cycled as part of the proof-testing of the complete system.

##### 2. Heat Content

Modifications to the calorimeter, welding fixture and other equipment were completed during this period. Heat content measurements of alumina were made, with the latest results tabulated in Table 401-I.

The heat contents are about 5% higher than those

TABLE 401-I

#### HEAT CONTENT OF ALUMINA

<u>Temperature (°C)</u>	<u>ΔH<sub>t</sub>-25° C (kcal/mole)</u>
1298	35.90
1431	40.74
1522	42.84
1598	45.15
1656	47.38
1781	51.90
1866	55.03
1973	58.95

previously reported<sup>1</sup>. The apparatus is being examined in an effort to account for this 5% variation in heat content values.

An operator is being trained for carrying out the heat content measurements. It is planned to put this equipment into "hot" operation prior to July 1, 1970. Some material from irradiated (U,Pu)C fuel elements is available for testing.

##### 3. Porosimeter

Work was begun on modification of a remotely operated mercury porosimeter to be used in obtaining the porosity of irradiated U-Pu fuels. That portion of the equipment involving the irradiated specimens will be located in the same containment box which houses the heat content apparatus. The pressurization and vacuum equipment will, of course, be located on a cart and used at the cell face.

##### 4. Shipping cask

Improvements to Shipping Cask DOT SP 5885 were made to overcome design and operational weaknesses. A reinforcing collar was welded to the top flange and then refaced to close tolerance to insure contact with the metal "V" seal ring.

On at least two occasions the flange on the plug has been deformed when the eyebolts (used to lift the cask) were not removed prior to removing the plug, as specified in the "Unloading Procedure". This problem has been obviated by adding a wide collar at the base of the lifting eyes. This collar overlaps the bolts in the plug and makes it necessary to remove the lifting eyes to expose all of the bolts. These bolts have to be removed before the small lifting eye can be used to

withdraw the plug.

This cask has been used thus far in making seven shipments to and from various AEC contractors.

#### 5. Other Equipment

Design work has started on the conversion of a commercial ultrasonic impact grinder to a remotely operated microsampling apparatus for taking small core samples from irradiated fuel.

Plastic containers to be used with the 7 in. transfer were put into service for disposing of radioactive wastes. The containers work well for their intended purpose. It was determined that it takes 200 lbs of force to remove a lid from the can. Since there is a glued point in the polycarbonate lids, which could separate during lid removal if poorly joined, a test fixture was designed and constructed to test each of the lids for strength. Each lid is tested to 350 lbs tensile strength before it is accepted for use. A chamber was also constructed for purging the air with argon prior to attaching the container to the alpha box. This development is a significant advance in the technology of remote transfer techniques.

### III. DP WEST FACILITY

(F. J. Fitzgibbon, M. E. Lazarus, C. D. Montgomery, J. R. Trujillo)

This facility which contains four hot cells is being modified to provide space and equipment for the nondestructive examination of irradiated fast reactor fuel pins. Equipment is being designed to examine fuel pins at a rate of 150 per year. Progress made on the major items during this Quarter is listed in the following sections.

#### A. Unloading and Handling

Purchase orders have been placed for the 25-ton hoist, the 3-ton remote hoist, and the manipulator crane bridge system. Delivery on all 3 items is scheduled for about July 1, 1970.

A job order has been issued for local fabrication of the cask transport cart which has a capacity of 23 tons. The cart will be pushed by fork lift from the unloading platform into the corridor area behind the cells.

A small hoist will be installed to permit unloading inserts from vertical casks. An intercell transfer

system for movement of pins between cells is being fabricated.

#### B. Profilometry

The electro-optical gauging system has been returned to the vendor for adjustments. The mechanical handling system and the lighting system for the pins are being fabricated.

An x-y coordinate positioning table has been received for use with the optical gauging head. Procurement has been initiated on the electronic read-out and recording systems.

#### C. Gamma Scanning

Modifications were made to the gamma scanning shield to accommodate new detectors. The mechanical portion of the scanning system is being fabricated. The encoders are scheduled for delivery in April.

Length and diameter standards are being prepared for dimensional calibration of the mechanical system. The standards consist of two  $^{60}\text{Co}$  cylinders of precise dimensions separated by a Dural rod of known length. The entire assembly is about 12 in. long; the dimension of both the  $^{60}\text{Co}$  cylinders and the Dural separator can be traced to NBS standards. With existing techniques the height of irradiated fuel columns can be determined with an accuracy of  $\pm 0.010$  in.

#### D. Macro-Photography

Various means have been investigated to obtain photographs of the exterior surfaces of pins at  $0^\circ$ ,  $120^\circ$ , and  $240^\circ$  orientations. Experiments were carried out with a two mirror system to obtain three views of a fuel element on one photograph.

A design is being prepared on a pin lighting and positioning system. The light will be provided by twenty fluorescent lamps and a 300-watt quartz-iodine lamp. Frontal illumination will be obtained by reflecting the light from the quartz-iodine lamp with a beam-splitting mirror. Design of the fixed focus camera and camera stand should be completed by May 1.

#### E. Other Operations

A system using a hot mineral oil bath was developed for removing Na and capsule cladding from irradiated pins without exposing the Na-coated pin to the air.

This technique has been successfully demonstrated on four irradiated pins.

A system for sampling the cover gas is essentially completed. Additional Baratron gauges and calibration standards have been ordered for this system. Improvements recently made to the fission gas sampling system in Cell 14 will be incorporated into the cover gas sampling system.

The twenty-two storage holes are being modified to hold the 61 in. long unencapsulated pins as well as the 40 in. long capsules. Preliminary critical calculations indicate that at least 12 typical pins could be safely stored in each of the holes.

Two Kollmorgen periscopes, ordered for detailed examination and photography, are expected to be received before June 1.

#### IV. METHODS OF ANALYSIS

##### Measurement of U and Pu

(J. W. Dahlby and G. R. Waterbury)

Controlled-potential coulometric titrations were shown previously to be satisfactory for measuring U and Pu in mixed oxide or carbide fuels having undergone burnups significantly less than 1%. The method gave high and erratic results on mixed oxide fuels having approximately 1% burnup. The difficulties were assumed to be caused, at least in part, by the hydrogen peroxide generated by the intense radioactivity of the sample solution. Removal of the peroxide from solution by reaction with peroxidase and catalase enzymes, addition of sulfamic acid, and fuming the samples with  $H_2SO_4$  immediately before the titration did not eliminate the bias. Reduction of the sample size to 1 mg decreased the bias to about 1%.

Further reduction of the bias in the Pu titration to 0.1% absolute was accomplished by a redox cycling technique. This involved repeated cycling of the Pu between the (III) and (IV) oxidation states until consecutive values for Pu obtained during either the coulometric reduction or oxidation agreed within 2  $\mu g$ . During the first redox cycle, the results of consecutive measurements differed by as much as 1 mg, and four or five cycles were required before the difference was reduced

to 2  $\mu g$ . By using this technique, the average obtained for Pu in the mixed oxide fuel having undergone 1% burnup was 22.2% as compared to 22.1% found in fuel from the same batch before irradiation.

A method for determining a reliable correction factor was developed to reduce the bias in the titration of U. A 1-mg sample was titrated in the usual way. Then the sample was left in the titration cell for a predetermined waiting period and retitrated. The length of the waiting period was adjusted to make the total time involved in this second titration equal to the time required for the first titration. Subtraction of the blank obtained by this second titration reduced the bias to 0.5 relative percent. An average of 65.9% was obtained for U in the mixed oxide fuel with 1% burnup as compared to 66.2% measured in the same batch of fuel before irradiation. Other techniques under consideration for improving the titration of U include (a) use of a glassy carbon working electrode instead of Hg and (b) redox cycling.

##### Gross Gamma Scanning

(J. Phillips and J. Deal)

Testing was completed on a simple gross gamma scanning system that was assembled to provide information quickly and non-destructively about areas of interest for further analyses in irradiated fuel elements. The system consisted of the existing scanning mechanism, slit, and lithium-drifted germanium detector of the high-resolution gamma scanner, and a new amplifier, single channel analyzer set to accept all gamma energies above a preset background, a scaler timer, and a printer readout. This simple scanner was satisfactory during testing and in gross gamma scanning of two irradiated fuel elements. It was possible to take data on an irradiated fuel element and obtain the gross gamma scan in one day. Measurements of fuel lengths with this system were accurate within 0.01 in. The gross gamma scanner complemented the high-resolution system for detailed gamma scanning and was used when a rapid gross gamma scan was required.

Components were received for the new high resolution system (Nuclear Data 50/50) which can be used for either gross gamma scanning or the various modes of

detailed gamma scanning. The components are being assembled for testing prior to installation in the DP West hot cell facility.

V. EXAMINATION OF UNIRRADIATED FUELS  
(K. A. Johnson, C. Baker, J. A. Leary)

Seven unirradiated pellets of  $U_{0.8}Pu_{0.2}C_{1+x}$  were examined for WARD. These specimens were typical samples from WARD Batches 535, 536, 539, 548, and 549. Pellet densities were determined, followed by metallography, microhardness, and electron microprobe examination. Results have been summarized in document CMB-11-9604 "Results of Examination of WARD Carbide Pellets, II," March 12, 1970. Copies were sent to AEC/RDT and to WARD.

VI. REQUESTS FROM DRDT

Examination of Irradiated Material  
(K. A. Johnson, E. D. Loughran (GMX-2),  
J. R. Phillips, J. W. Schulte, J. F. Torbert  
(GMX-1), G. R. Waterbury)

Atomics International

Examinations of materials from irradiation test experiment NRX-101 were completed with the receipt by AI of the burnup results obtained at INC. Proper disposal of the AI materials was started.

Battelle Northwest Laboratory

A report describing the microprobe examination of a specimen from fuel pin BNW-1-11 was forwarded to DRDT and BNWL.

LASL (K-Division)

Experiments OWREX 12 and OWREX 13 were disassembled and visually examined. Experiment OWREX 14 was received; nondestructive testing will be started in early April.

One fuel-clad sample from OWREX 12 and four fuel-clad samples from OWREX 13 were examined metallographically. The examination, conducted in an Ar atmosphere, consisted of the following: macrophotography, alpha and beta-gamma autoradiography, and optical metallography.

Nuclear Materials and Equipment Corporation

The following tests and measurements were completed on NUMEC B-1 and NUMEC B-9 capsules and pins; radiography, diameter measurements of the

capsules, analysis of cover gas from the capsule, macrophotography and profilometry. Gross gamma scanning was completed on the NUMEC B-1 capsule.

In addition to those tests conducted on NUMEC B-11 last Quarter, the following operations were carried out during this period; gross (and detailed) gamma scanning, analysis of cover gas sample from capsule, analysis of fission gas sample from pin, macrophotography, and 2 samples each taken for density and burnup determinations.

Removal of the capsule cladding and sodium, and sectioning of the pin were carried out in an Ar atmosphere.

Six specimens of fuel-clad were examined in an Ar atmosphere using the following capabilities: alpha autoradiography, beta-gamma autoradiography, and macrophotography. Optical metallography on these specimens was not completed during this Quarter.

A section of capsule cladding in the vicinity of the breach in the pin cladding was slit longitudinally and the sodium removed by washing with Dowanol EB and alcohol. Detailed photographs of the interior surface of the cladding were made using the Kollmorgen periscope.

Data reports were forwarded to NUMEC and DRDT when phases of the work were completed.

United Nuclear Corporation

Ten fuel pins (or sections) from United Nuclear were examined during this period. The types of examinations or operations conducted on these fuel pins are as follows:

UNC-87, -89, and -90

Electron microprobe examinations of UNC-87 and -90 were completed, and the data for UNC-87 was forwarded to UNC and DRDT. Preparation of the data report for UNC-90 and the examination of a specimen from UNC-89 are in progress. Radiochemical analyses of eleven previously dissolved iron, flux-monitor wires were reported as before.

Metallographic operations carried out during this period consisted of microphotography on 4 Nb disk specimens and two fuel-clad specimens from UNC-90. A replica

of the surface of one of the fuel-clad specimens from UNC-90 was also prepared.

#### UNC-101

This capsule was received on February 5, 1970, and the examinations or operations completed during the Quarter are: gross gamma scanning, radiography with the Betatron, measurement of capsule diameter, profilometry on pin, analysis of cover gas sample from capsule and fission gas sample from pin, macrophotography of fuel pin surface, and disassembly in an Ar atmosphere.

Metallographic examination, carried out during this Quarter, consisted of: alpha and beta-gamma autoradiography, macrophotography, and microphotography on four fuel-clad specimens. The specimens were also prepared in an Ar atmosphere.

#### UNC-81, -82, and -83

These capsules were received on October 29, 1969. The examinations or operations carried out during this period are as follows: analysis of cover gas (UNC-82 and -83) from the capsule; analysis of fission gas; macrophotography of pin surface; profilometry; density determinations on two samples from each pin; dissolution of three iron, flux-monitor wires and radiochemical analysis for absolute counting rates of  $^{54}\text{Mn}$ ; and two burnup samples from each pin were packaged for shipment to Idaho Nuclear for analysis.

One Nb disk and 4 fuel-clad specimens from UNC-81, five fuel-clad specimens from UNC-82, and six fuel-clad specimens from UNC-83 were examined metallographically. The following examinations were carried out on each sample: alpha and beta-gamma autoradiography, macrophotography, and microphotography. Replicas were prepared of one fuel-clad specimen from each of the three fuel pins.

#### UNC-84, -85, and -86

These capsules were received on March 18, 1970. The tests conducted during this Quarter were radiography with the Betatron and diameter measurements on the capsules. Gross gamma scanning was completed on UNC-86 only.

Data reports were forwarded to DRDT and UNC

as phases of the work were completed.

#### Westinghouse (WARD)

Analyses of gross and detailed gamma scanning data from three capsules (W-1-G, W-2-G, and W-3-G) were completed and data reports were sent to WARD.

A sample of unirradiated aluminum-cobalt wire from the same wire used as a flux monitor on the three capsules was sent to ANL (Illinois).

#### VII. REFERENCES

1. A. E. Ogard, Quarterly Status Report on the Advanced Plutonium Fuel Program, July 1 to September 30, 1969, LA-4307-MS, p. 26.

PROJECT 462

SODIUM TECHNOLOGY

Person in Charge: D. B. Hall  
Principal Investigator: J. C. Biery

All work on the Sodium Technology program will be discontinued at the end of FY-1970, for it is not funded beyond that time. Phaseout activities, including disposition of equipment, has begun. Final reports on the Sodium Technology work will be included in the Fourth Annual Report on the Advanced Plutonium Fuels Program which will be issued at the end of the current fiscal year.

PROJECT 463  
CERAMIC PLUTONIUM FUEL MATERIALS

Person in Charge: R. D. Baker  
Principal Investigator: J. A. Leary

I. INTRODUCTION

The principal goals of this project are to prepare pure, well characterized plutonium fuel materials, and to determine their high temperature properties. Properties of interest are: (1) thermal stability, (2) thermal expansion, (3) thermal conductivity, (4) phase relationships by differential thermal analysis, (5) structure and phase relationships by X-ray diffraction, high temperature X-ray diffraction, neutron diffraction and high-temperature neutron diffraction, (6) density, (7) hardness and its temperature dependence, (8) compatibility, including electron microprobe analysis, and (9) compressive creep (deformation).

II. SYNTHESIS AND FABRICATION

(R. Honnell, H. Moore, R. Walker, C. Baker, W. Hayes)

A. Materials for Properties Measurements

In support of physical properties measurements, a number of different carbide compositions were synthesized and fabricated into well characterized test specimens. A brief description of the compositions and areas of interest follows:

1. To further elucidate specific areas of the Pu-C phase diagram, approximately 10 different compositions were alloyed and fabricated into DTA test specimens. Compositions of interest were bounded by the sesquicarbide-dicarbide and the monocarbide compositions.

2. To obtain thermodynamic data on the Pu-C system from EMF measurements, test specimens were

sintered and characterized from  $\text{PuC}_{0.82}$ ,  $\text{PuC}_{0.90}$ , and  $\text{PuC}_{1.5}$  powders.

3. Approximately 500 grams of material was alloyed to a nominal composition of  $(\text{U}_{0.8}\text{Pu}_{0.2})\text{C}_{1.0}$  for the purpose of comminuting to powder and sintering to compressive creep and thermal conductivity specimens.

4. Powders of  $(\text{U}_{0.84}\text{Pu}_{0.16})\text{C}_{2.002}$  and  $(\text{U}_{0.4}\text{Pu}_{0.36})\text{C}_{2.008}$  were synthesized for powder X-ray diffraction studies.

B. Materials for Irradiation and Compatibility Experiments

Fifty-four pellets of  $^{233}\text{U}_{0.8}\text{Pu}_{0.2}\text{C}$  are characterized and available for fuel pin loading. Material is in progress to meet the 65 pellet fuel loading requirement with 10 spare pellets. A considerable number of pellets have been rejected because of the appearance of a grain boundary phase analyzed as being plutonium rich with significant amounts of iron, nickel, silicon, and chromium. The silicon impurity was traced to the U-233 feed metal, and corrective measures were taken in the uranium process metallurgy to reduce the silicon contamination. Pellets recently alloyed from low silicon uranium are free from grain boundary inclusions as determined by metallographic examination.

The use of U-233 in (U, Pu)C pellets has not introduced a serious radiation handling problem at the quantities employed, i. e., 150-gram ingots of newly

separated metal. For example, the gamma activity of a (U, Pu)C button containing approximately 60 grams of U-233 attained a level of 175 mr/h at contact after 78 days starting from an initial activity of 15 mr/h.

### III. PROPERTIES

#### 1. Differential Thermal Analysis

(J. G. Reavis, L. Reese)

Determination of temperatures of melting and of phase transformations in the Pu-C system by use of differential thermal analysis techniques has continued. Two samples of irradiated  $UO_2$ -25%  $PuO_2$  have also been investigated by application of DTA in the Hot Cells.

Transformations in the Pu-C System: Differential thermal analysis observations have been completed on 10 additional compositions over the range  $PuC_{0.70}$  -  $PuC_{1.85}$ . As reported previously, DTA does not give precise values of liquidus temperatures ( $\pm 20^\circ C$ ). Consequently, these temperatures must be determined by quenching samples from selected temperatures and examining them for complete liquid formation. Results of the observations are listed in Table 463-I. The liquidus values listed here are in fair agreement with the currently-accepted version of the Pu-C diagram, but the thermal arrests at  $1590^\circ C$  listed here differ significantly from those to be expected from the diagram. Additional compositions must be observed, however, before the diagram can be redrawn.

Table 463-I

TRANSFORMATION TEMPERATURES OF  
PuC COMPOSITIONS

Atomic Ratio, C/Pu	Arrest Temps., $^\circ C$	Liquidus, $^\circ C$
0.72	—	$1690 \pm 15$
0.77	—	$1675 \pm 25$
0.83	1585	$1670 \pm 20$
0.86	1595	$1685 \pm 10$
0.92	1590	$1735 \pm 20$
0.97	1590	$1720 \pm 20$
1.01	1590	$1780 \pm 20$
1.04	1590	$1785 \pm 20$
1.07	1595	$1810 \pm 20$
1.85	1660, 2015	$2235 \pm 15$

Observations of Irradiated  $UO_2$ -25%  $PuO_2$ : Two samples of  $UO_2$ -25%  $PuO_2$  irradiated to a level of  $\sim 9000$  MWD/T in EBR-II have been studied by DTA. Both samples were taken from the same fuel pin. The

samples were contained in W crucibles covered by loose-fitting W lids which had pyrometric sight holes in the center. The furnace was filled with Ar at about 0.5 atm pressure during thermal cycling. As the samples were heated, a film formed on the cooler parts of the furnace, including the window through which the light beam to the pyrometer and the DTA sensors emerged. This necessitated frequent interruption of thermal cycling for window changing and gave uncertainties in temperatures of the order of  $100^\circ$  at times because of the uncertainty of thickness of the film. Qualitative measurements showed the presence of significant amounts of  $\beta$ - $\gamma$  activity in the material deposited on the window.

Arcing of the induction-heated furnace was a more serious problem than usual. It is believed that the presence of the volatile material aggravated this problem. Arcing leads to surges and drops of power input to the furnace so that the thermal cycles are non-linear and the identification of valid arrests in temperature and  $\Delta T$  curves becomes very difficult.

Because of these experimental difficulties, the uncertainties in temperatures of arrests are larger than those usually encountered in DTA investigations on unirradiated fuel. The sensitivity of the measurements was also adversely affected by the non-linearity of the T and  $\Delta T$  curves. It is estimated that a transformation must involve release or absorption of the order of 10 cal/g of fuel over a temperature range of  $10^\circ$  or less to be detected under these conditions. This type of DTA apparatus normally is more sensitive by almost an order of magnitude.

No solid/solid transformations were detected in either of the fuel samples. The observed solidus and liquidus values are compared in Table 463-II with solidus and liquidus temperatures observed for an unirradiated sample of  $UO_2$ -25%  $PuO_2$  in the same apparatus. Although there appears to be a trend toward higher values of the melting point in the irradiated samples, this trend is less than the uncertainties of measurement.

Irradiated sample No. 1 was photographed after heating to  $2775 \pm 25^\circ$  and is shown by Fig. 463-1. At

Table 463-II  
 SOLIDUS AND LIQUIDUS TEMPERATURES OF  
 $UO_2$ -25%  $PuO_2$

Sample	Solidus, °C	Liquidus, °C
Unirradiated	2675 ± 20	2775 ± 20
Irradiated No. 1	2750 ± 50	2825 ± 50
Irradiated No. 2	2680 ± 25	—

this time the sample was found to have sintered so that the granules stuck together but there was no slumping or other indication of macro liquid phase formation. After this sample was heated to  $2860 \pm 25^\circ$  it was found to have been completely liquid as is shown by Fig. 463-2.

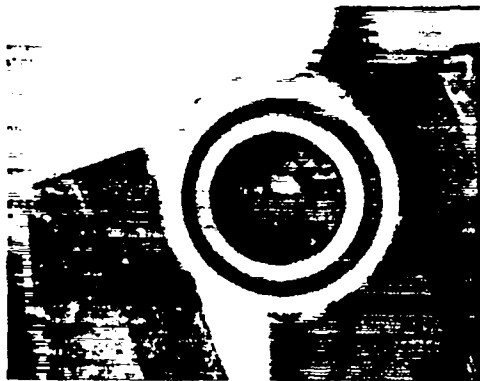


Figure 463-1. Irradiated  $UO_2$ -25%  $PuO_2$  after heating to  $2775 \pm 25^\circ C$  (3/4 in. dia crucible)



Figure 463-2. Irradiated  $UO_2$ -25%  $PuO_2$  after heating to  $2860 \pm 25^\circ C$  (3/4 in. dia crucible)

The second sample was inspected after heating to  $2820 \pm 25^\circ$  and again after heating to  $2900 \pm 50^\circ$ . At  $2820 \pm 25^\circ$  the sample had slumped, showing considerable penetration into the solid plus liquid region, but melting was not complete. At  $2900 \pm 50^\circ$  the sample was completely liquid.

## 2. Room Temperature X-ray Diffraction (C. W. Bjorklund)

The characterization of plutonium fuel materials by X-ray powder diffraction techniques has continued. The results have been incorporated elsewhere in appropriate sections of this report.

Evaluation of a precision linear comparator for measuring powder diffraction films has been continued. This instrument is capable of reading directly to 0.001 mm compared to 0.05 mm for a desk top film reader.

In previous reports, an equation was developed to calculate the relative lattice expansion of self-irradiation damaged  $PuO_2$  as a function of time and temperature over the temperature range  $-200^\circ$  to  $400^\circ C$ . A modification of this equation could be used to calculate a thermal annealing curve for radiation damaged  $PuO_2$  over the same temperature range, but the curve leveled off prematurely when an attempt was made to extrapolate it to higher temperatures. Previous difficulties have now been overcome in calculating new parameters for the original equation to include arbitrary data showing negligible lattice expansion at  $1000^\circ C$ . However, as suspected, the agreement obtained between the experimental data and the calculated curves at the lower temperatures is not as good when the new parameters are used. The calculated annealing curve is somewhat improved at the higher temperatures when the new parameters are used, but not to the extent desired. One of the parameters in the original equation includes an activation energy term which was assumed to be representative of a single first-order annealing process occurring over the entire temperature range, or, as is more likely, an average value for several first order annealing processes. The results described above support the hypothesis that this activation energy term is responsible for the failure of the equation to

apply over the entire temperature range from  $-200^{\circ}$  to  $1000^{\circ}\text{C}$ . More likely, several annealing processes with different activation energies occur simultaneously at rates which differ with temperature as suggested by Kelley (B. T. Kelley, "Irradiation Damage to Solids", Pergamon Press, (1966) p. 180). A single value probably cannot be selected as an average value applicable over the entire temperature range.

### 3. High Temperature X-ray Diffraction (J. L. Green, K. Walters)

The investigation of the high temperature crystallographic properties of materials associated with the carbon rich fields of the U-Pu-C phase diagram is continuing.

An independent determination of the sesquicarbide to cubic dicarbide transformation temperature has been completed for  $(\text{U}_{0.65}\text{Pu}_{0.35})\text{C}_2$ . The transformation was observed to occur at  $1735 < T < 1750^{\circ}\text{C}$ . Differential thermal analysis data was not available for this particular composition; therefore, a sample was prepared and the transformation temperature was measured using that technique. The transformation temperature measured was  $1740 \pm 10^{\circ}\text{C}$  which is in excellent agreement with the value reported above. During the DTA investigation, an attempt was made to obtain a corroborative observation of the bct to fcc dicarbide transformation that has been observed at  $1550^{\circ}\text{C}$  in diffraction studies. No thermal arrest was observed near that temperature. It was estimated that an energy release corresponding to approximately 5% of that associated with the dicarbide to sesquicarbide transformation would have been detectable. The transformation energy for the bct to fcc dicarbide transformation is estimated to be approximately 50% of that for the decomposition reaction; therefore, 10% of the sample would have to be involved before the bct to fcc transformation would be detectable. Diffraction studies have indicated that only approximately 8% of the material at this composition is involved in the transformation; therefore, it appears that the thermal effects are not large enough to be observable. An independent identification of this feature would be desirable; however, it does not appear that it will be possible

to do so using DTA.

Cooling a well crystallized sample of fcc  $(\text{U}_{0.65}\text{Pu}_{0.35})\text{C}_2$  from  $1850^{\circ}\text{C}$  to room temperature in approximately 15 sec yielded a quenched sample of essentially 100% bct dicarbide. Only traces of the strongest sesquicarbide lines were observed. A least squares fit of the diffraction data yielded the following lattice parameters:

$$a_0 = 3.5528 \pm 0.0008 \text{ \AA}$$

$$c_0 = 6.023 \pm 0.003 \text{ \AA}$$

where the error limits represent the 95% confidence interval with respect to internal consistency. For comparative purposes, the lattice parameter data from earlier quenching studies (arc melting and DTA) were reviewed and least squares fitted to linear functions of composition. The  $a_0$  reported above is smaller by approximately  $0.002 \text{ \AA}$  than that calculated from the fitted equation while the  $c_0$  values are essentially identical. This sample was subsequently used to study the effect of low temperature annealing on bct dicarbide. Annealing for 2.25 hr at power levels less than 75% of that required to produce the first observable color in the sample area had no effect on the bct pattern. Annealing for 45 minutes with the sample just observably red ( $\sim 500^{\circ}\text{C}$ ) resulted in the decrease of the bct line intensities to essentially the values observed using slowly cooled samples. Annealing for an additional 5.5 hr at that power caused minor decreases in the bct line intensities; however, the interpretation of these changes was complicated by what appeared to be sample oxidation. It is not possible, therefore, to decide whether or not the small residual amount of bct dicarbide is stable at this temperature; however, it may be concluded that amounts in excess of this are unstable.

### 4. Thermodynamic Properties of Plutonium Compounds by Electromotive Force Techniques (G. M. Campbell)

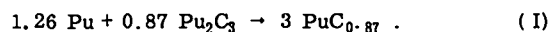
Three cells of the type



where the anode had a C to Pu atomic ratio of 1.066 were monitored galvanostatically.<sup>(1)</sup> Initial potentials were sufficiently negative with respect to the standard

Pu<sup>3+</sup>/Pu<sup>4+</sup> potential (>600 mV) to indicate a negligible current from this source. Voltammetric analysis confirmed this. After two weeks, however, these analyses indicated a rapid increase in Pu<sup>4+</sup> levels which was accompanied by a pronounced positive drift in the cell emf. These effects were in accordance with those expected with a mixed oxidation state electrolyte. Equilibrium potentials after the rapid drift were stable but nearly the same as those of Pu<sub>2</sub>C<sub>3</sub> + C electrodes. Since these potentials were too positive to correlate with the initial potentials a solid state surface composition change was expected. Chemical analysis of these electrodes indicated the C to Pu atomic ratio had increased to 1.8.

Since the current from the Pu<sup>3+</sup>/Pu<sup>4+</sup> equilibrium during the initial equilibration is negligible, these potentials can be used to calculate the free energy of the reaction



Data from two of these cells are given in Table 463-III.

Table 463-III

EMF DATA FROM CELL CONTAINING ELECTRODES OF PuC<sub>0.87</sub> + Pu<sub>2</sub>C<sub>3</sub> AGAINST Pu(l)

Cell	Emf, V	Temp., °K
1	0.1393	958.5
1	0.1343	963.5
1	0.1408	978.1
1	0.1381	986.7
1	0.1362	991.2
1	0.1353	980.2
1	0.1301	1000.7
1	0.1342	993.1
1	0.1391	1012.4
2	0.1308	957.9
2	0.1330	951.3
2	0.1325	967.0
2	0.1300	991.8
2	0.1311	983.5
2	0.1399	951.6

A least squares analysis gives the potential

$$E = 0.1482 - 0.000135 T (\pm 0.0037) \text{ V.} \quad (\text{II})$$

The partial molar free energy of Pu is

$$\Delta \bar{G}_T = -10.25 + 0.00093 T \text{ kcal/mole.} \quad (\text{III})$$

This can be combined with the results of studies made previously which indicated that at these temperatures the

free energy of formation of Pu<sub>2</sub>C<sub>3</sub> is

$$\Delta G_T^\circ = -42.0 + 0.012 T \text{ kcal/mole.} \quad (\text{IV})$$

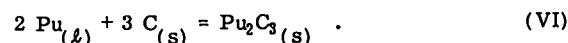
This results in the free energy of formation of PuC<sub>0.87</sub> as

$$\Delta G_T^\circ = -16.48 + 0.00387 T \text{ kcal/mole.} \quad (\text{V})$$

Since there is thermal data<sup>(4)</sup> available for PuC<sub>0.87</sub>,

it is possible to make a third law calculation of ΔH.

Using ΔG<sub>1000</sub><sup>o</sup> = -12.6 and S<sub>1000</sub><sup>o</sup> = 32.6 leads to ΔS<sub>1000</sub><sup>o</sup> = +0.1 eu and ΔH<sub>1000</sub><sup>o</sup> = -12.5 kcal/mole or ΔH<sub>298</sub><sup>o</sup> = -10.8 kcal/mole for PuC<sub>0.87</sub>. Using ΔS<sub>1000</sub><sup>o</sup> for reaction (I) as -0.93 eu (eq. III) S<sub>1000</sub><sup>o</sup> for Pu<sub>2</sub>C<sub>3</sub> becomes 71.7 eu, and using the free energy of formation of Pu<sub>2</sub>C<sub>3</sub> from emf measurements of -30 kcal at 1000<sup>o</sup>K, ΔS<sub>1000</sub><sup>o</sup> = -0.4 and ΔH<sub>1000</sub><sup>o</sup> = -30.4 for the reaction



ΔH<sub>298</sub><sup>o</sup> = -27 kcal/mole Pu<sub>2</sub>C<sub>3</sub> for this reaction. The results are in good agreement with extrapolated tensimetric data. These experiments indicate that large potential shifts should be avoided if possible during equilibration. A pre-electrolysis step may be necessary in some cases. One or two more Pu-C compositions will be examined.

#### 5. Mass Spectrometric Studies of the Vaporization of Pu Compounds (R. A. Kent)

##### The Pu-C System

The study of the vaporization behavior of the Pu-C system as a function of composition and temperature is being continued. During this quarter, a total of nine experiments were performed on samples ranging in composition from PuC<sub>0.7</sub> to PuC<sub>2</sub>. The results from these experiments when combined with data obtained previously<sup>(2)</sup> yield the following information about the vaporization behavior of this system.

There are three regions of the Pu-C phase diagram which give rise to invariant but not congruent vaporization:

- (1) Pu<sub>2</sub>C<sub>3</sub> + C
- (2) PuC<sub>2</sub> + C
- (3) PuC + Pu<sub>2</sub>C<sub>3</sub>

The vaporization behavior of the Pu-C system may be described as follows. As one adds C to Pu(l) the

pressure of Pu(g) at a given temperature decreases as the Pu activity is lowered. When the low carbon boundary of the monocarbide is reached, the Pu(g) pressure falls sharply. As one continues to heat the sample and to add C, the monocarbide reacts to form Pu(g) and sesquicarbide. The Pu(g) pressure remains invariant so long as both the monocarbide and sesquicarbide are present as solid phases. When the low carbon boundary of the sesquicarbide is reached the Pu(g) pressure falls sharply. The sesquicarbide on heating, gives off Pu(g) with free carbon appearing in the condensate. Again, the Pu(g) pressure is invariant so long as both sesquicarbide and free carbon are present. Above 1660°C the sesquicarbide transforms to the dicarbide with a resultant change in Pu(g) pressure. Vapor pressure values for various compositions at 1700°K are listed in Table 463-IV.

Table 463-IV  
PRESSURE OF Pu(g) AT 1700°K AS A FUNCTION OF COMPOSITION

Composition of Condensate	Pu(g) Pressure, atmospheres
Pu(l)	$4.75 \times 10^{-6}$
PuC <sub>0.71</sub> (s)	$2.71 \times 10^{-6}$
PuC <sub>0.76</sub> (s)	$2.41 \times 10^{-6}$
("PuC" + Pu <sub>2</sub> C <sub>3</sub> )(s)	$9.76 \times 10^{-7}$
(Pu <sub>2</sub> C <sub>3</sub> + C)(s)	$2.28 \times 10^{-8}$

Pu<sub>2</sub>C<sub>3</sub> + C

Above the two phase condensate Pu<sub>2</sub>C<sub>3</sub> + C, the Pu(g) pressure is given by  
 $\log P_{\text{Pu}}(\text{atm}) = (4.402 \pm 0.082) - 20474 \pm 151/T^{\circ}\text{K}$ ,  
 (1545-1927°K). (1)

When the free energy expression for the decomposition of Pu<sub>2</sub>C<sub>3</sub> is combined with that for the vaporization of Pu<sup>(3)</sup> we have

$$\text{Pu(g)} + 1.5\text{C(s)} = \text{PuC}_{1.5}\text{(s)};$$

$$\Delta G_{1850} = -93,685 + 20.14 T \quad (2)$$

$$\text{Pu(l)} = \text{Pu(g)};$$

$$\Delta G_{1850} = 80,176 - 22.64 T \quad (3)$$

$$\text{Pu(l)} + 1.5 \text{C(s)} = \text{PuC}_{1.5}\text{(s)};$$

$$\Delta G_{1850} = -13,509 - 2.50 T \quad (4)$$

As no high temperature C<sub>p</sub> data exist for PuC<sub>1.5</sub>(s), thermal functions were estimated from known values for PuC(s)<sup>(4)</sup> and C.<sup>(5)</sup> Equation (4) then reduces to yield

$$\Delta H_{f298}^{\circ} = -12.74 \pm 2.00 \text{ kcal/mole and } \Delta S_{f298}^{\circ} = +5.70 \pm 1.50 \text{ eu. The value of } S_{298}^{\circ} \text{ is calculated to be } 20.94 \text{ eu.}$$

This value of S<sub>298</sub><sup>o</sup> was employed to calculate the free-energy functions for PuC<sub>1.5</sub>(s) used to generate the third law values presented in Table 463-V.

Table 463-V  
THIRD LAW RESULTS FOR THE DECOMPOSITION OF PuC<sub>1.5</sub>(s)

Temp., °K	Pu Pressure, atmosphere	-Δ <sub>f</sub> ef (eu) for reaction (2)	ΔH <sub>298</sub> (kcal/mole) for reaction (2)	ΔH <sub>f298</sub> kcal/mole
1500	$5.65 \times 10^{-10}$	21.51	95.74	-12.74
1600	$4.03 \times 10^{-9}$	21.44	95.75	-12.75
1700	$2.28 \times 10^{-8}$	21.37	95.77	-12.77
1800	$1.07 \times 10^{-7}$	21.29	95.76	-12.76
1900	$4.23 \times 10^{-7}$	21.24	95.78	-12.78
				-12.76

PuC<sub>2</sub> + C

The dicarbide decomposes to Pu(g) and free C with the Pu(g) pressure given by

$$\log P_{\text{Pu}}(\text{atm}) = (3.791 \pm 0.168) - 19293 \pm 341/T^{\circ}\text{K},$$

$$(1934-2200^{\circ}\text{K}). \quad (5)$$

When the vapor pressure data for the decomposition of PuC<sub>2</sub>(s) are combined with those for the vaporization of Pu<sup>(3)</sup> we have

$$\text{Pu(g)} + 2 \text{C(s)} = \text{PuC}_2\text{(s)};$$

$$\Delta G_{2026} = -88,281 + 17.35 T \quad (6)$$

$$\text{Pu(l)} = \text{Pu(g)};$$

$$\Delta G_{2026} = 80684 - 22.91 T \quad (7)$$

$$\text{Pu(l)} + 2 \text{C(s)} = \text{PuC}_2\text{(s)};$$

$$\Delta G_{f2026} = -7,597 - 5.56 T \quad (8)$$

When equations (4) and (8) are combined, we have for the transition from sesquicarbide to dicarbide

$$\text{PuC}_{1.5}\text{(s)} = \text{Pu(l)} + 1.5 \text{C(s)}, \Delta G = 13,509 + 2.50 T$$

$$\text{Pu(l)} + 2 \text{C(s)} = \text{PuC}_2\text{(s)}, \Delta G = -7,597 - 5.56 T$$

$$\text{PuC}_{1.5}\text{(s)} + 0.5 \text{C(s)} = \text{PuC}_2\text{(s)}, \Delta G = 5,912 - 3.06 T \quad (9)$$

The transition temperature is calculated to be 1932°K (1659°C).

Some of the vapor pressure data taken above Pu<sub>2</sub>C<sub>3</sub> + C and PuC<sub>2</sub> + C are presented in Fig. 463-3.

PuC + Pu<sub>2</sub>C<sub>3</sub>

The Pu(g) pressure above monocarbide-sesquicarbide mixtures is given by

$$\log P_{\text{Pu}}(\text{atm}) = (5.130 \pm 0.042) - 18939 \pm 70/T^{\circ}\text{K},$$

$$(1450-1848^{\circ}\text{K}). \quad (10)$$

There is some uncertainty as to the actual monocarbide composition at high temperatures, but the limits probably are between PuC<sub>0.86</sub> and PuC<sub>0.91</sub>. For

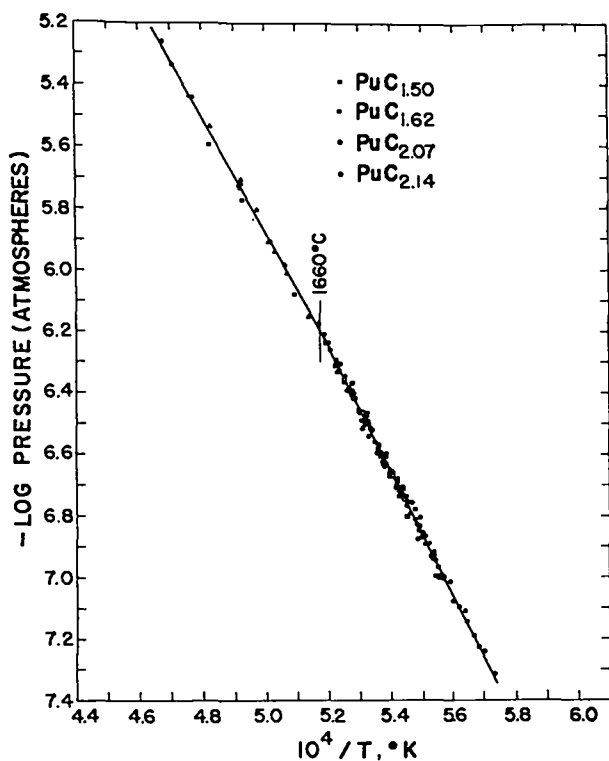
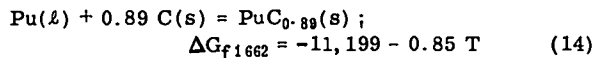
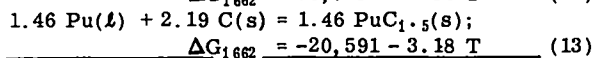
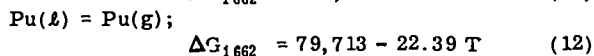
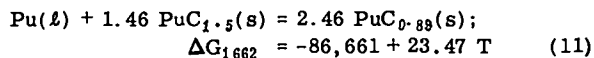


Figure 463-3. Plutonium gas pressure above plutonium sesquicarbide and plutonium dicarbide.

this work we take the composition to be  $\text{PuC}_{0.89}$ . When the vapor pressure data for the decomposition of the monocarbide are combined with those for the decomposition of the sesquicarbide and the vaporization of Pu metal, <sup>(2)</sup> we have



When eq (14) is reduced to 298°K using known functions for  $\text{Pu}(l)$ , <sup>(3)</sup>  $\text{C}$ , <sup>(5)</sup> and  $\text{PuC}$  <sup>(4)</sup>, we obtain for  $\text{PuC}_{0.89}(s)$ ,  $\Delta H_{f298}^{\circ} = -10.62 \pm 2.00$  kcal/mole and  $\Delta S_{f298}^{\circ} = +2.91 \pm 1.50$  eu. The value of  $S_{298}^{\circ}$  is calculated to be 17.32 eu.

The free-energy functions estimated for  $\text{PuC}_{1.5}(s)$  were combined with the known functions for  $\text{Pu}(l)$  <sup>(2)</sup> and  $\text{PuC}$  <sup>(3)</sup> to generate the third law values listed in Table 463-VI.

Table 463-VI  
THIRD LAW RESULTS FOR THE DECOMPOSITION OF  $\text{PuC}_{0.89}(s)$

Temp., °K	Pu Pressure, atmospheres	$-\Delta f$ (eu) for reaction (11)	$\Delta H_{298}^{\circ}$ (kcal/mole) for reaction (11)	$\Delta H_{f298}^{\circ}$ , $\text{PuC}_{0.89}$ kcal/mole
1500	$3.19 \times 10^{-4}$	26.78	90.62	-10.67
1600	$1.96 \times 10^{-4}$	25.59	90.63	-10.68
1700	$9.76 \times 10^{-5}$	25.43	90.62	-10.67
1800	$4.06 \times 10^{-5}$	25.30	90.65	-10.68

Some of the vapor pressure data taken above monocarbide-sesquicarbide mixtures are presented in Fig. 463-4.

The vapor pressure data indicate that the low-carbon phase boundary for the sesquicarbide curves to the left at high temperatures passing through  $\text{PuC}_{1.45}$  at 1500°C,  $\text{PuC}_{1.41}$  at 1550°C and  $\text{PuC}_{1.31}$  at 1580°C.

#### 6. High Temperature Calorimetry

(A. E. Ogard)

There are three types of drop calorimeters that are used for the determination of high temperature heat contents; each with its own problems. The isothermal

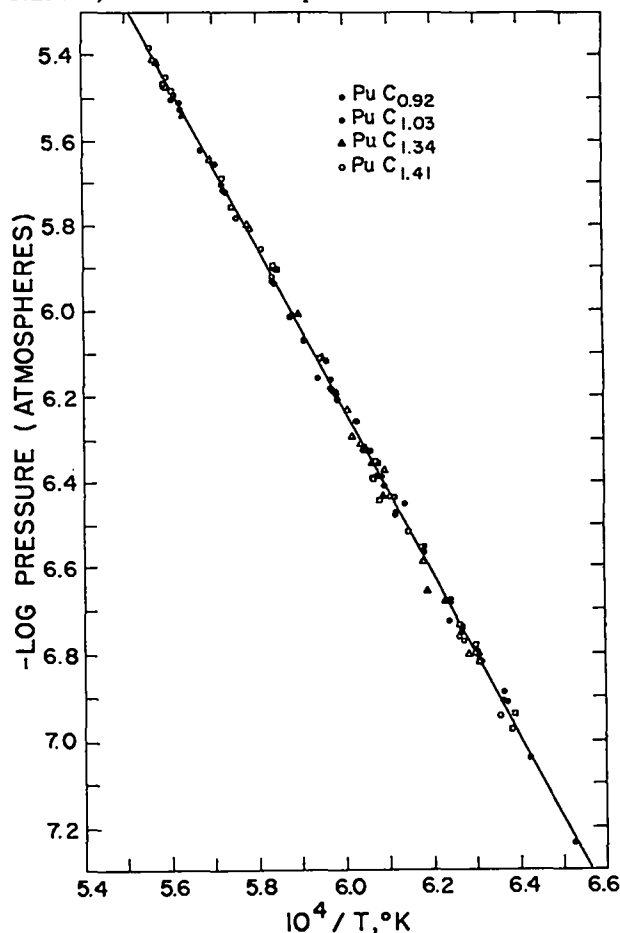


Figure 463-4. Plutonium gas pressure above plutonium monocarbide plus plutonium sesquicarbide

or ice calorimeter is difficult to use with very high temperature furnaces and a correction for heat leak to the surroundings is made in the calculations. An adiabatic calorimeter supposedly eliminates heat leak corrections but the error in controlling the adiabatic conditions may be as great as in the correction itself. The third method is the isoperibol or copper block calorimeter in which a correction is made for heat leakage to the surroundings. As reported previously, a copper block calorimeter is used in this work on plutonium-containing reactor fuel materials.

In a copper-block drop calorimeter the change in temperature of the copper block due to an unknown quantity of heat being added is found by adding a correction term to the observed increase in temperature of the copper block.

$$\Delta\theta = (\theta_m - \theta_o) + \int_{t_o}^{t_m} k(\theta - \theta_k) dt \quad (1)$$

where  $\theta_o$  and  $\theta_m$  are the temperatures at the beginning and end of heating,  $t_o$  and  $t_m$  are the times of heating,  $k$  is the cooling constant of the calorimeter and  $\theta_k$  is the temperature of the isothermal surroundings.

The normal procedure is to first electrically calibrate the calorimeter. A measured amount of heat is supplied electrically. This amount of heat is divided in the corrected temperature change,  $\Delta\theta$ , from equation (1) to give the calibration constant of the calorimeter. The temperature rise of the copper block is kept to less than 3°C and the calorimeter is operated in vacuum so that Newton's law of cooling applies. The electrical energy is also supplied to the calorimeter at relatively slow rates compared to actual drops. If care is exercised a precision of better than ± 0.1% can be obtained.

In a high temperature drop calorimeter (1000 to 3000°C) it is not always easy to keep the sample size small so that the temperature rise is less than 3°C. In this work temperature rises of up to 10°C occur. At these large temperature rises Newton's law of cooling may not be applicable even in vacuum. Therefore, it seems necessary to make a thorough study of the factors entering into the calibration. Also it is necessary to

increase the rate of heating during calibration to approach the very rapid rate of heating encountered in the actual drops.

By heating the calorimeter to  $\Delta\theta \approx 10^\circ\text{C}$  and then allowing it to cool, the cooling constant  $k$  was determined. Up to  $\Delta\theta = 5^\circ\text{C}$ , the cooling constant  $k = 0.00155 \text{ min}^{-1}$ ; above  $\Delta\theta = 5^\circ\text{C}$   $k = 0.00155 + 0.000015 \Delta\theta$ . In argon the cooling constant is expressed by the equation  $k = 0.00155 + 0.000060 \Delta\theta$  over the range of  $\Delta\theta = 0$  to  $10^\circ\text{C}$ . If a 0.050 in. thick aluminum convection shield is used around the calorimeter block  $k = 0.00062 \text{ min}^{-1}$ .

Table 463-VII shows the most recent calibrations of the high temperature calorimeter. The convection shield was not used.

The calibration constant calculated from equation (1) appears to be independent of the rate of heating and total heat supplied so long as the time is kept constant. However, as the length of time of heating is increased, the calibration constant also increases. Empirically the constant can be also made independent of the time of heating by using  $2k$  for the cooling rate before substituting in equation (1). These results are shown in the last column of Table 463-VII and are about 2% lower than the results from equation (1). The departure from Newton's law of cooling may be due to the non-equilibrium conditions existing in the calorimeter block during rapid heating. It takes ~90 min after the electrical heating is stopped before the copper block reaches true equilibrium as shown by the cooling rate equal to  $k$ .

These results point out that although the precision of a high temperature calorimeter is very good its actual accuracy is somewhat unknown. Further calibrations are necessary, especially in argon. Similar results should be obtained when the calorimeter is run in argon as in vacuum if the cooling correction is correct.

#### 7. Transport Properties (K. W. R. Johnson, J. F. Kerrisk) Electrical Resistivity

A method of measuring electrical resistivity of disc shaped samples has been investigated (L. J. van der Pauw, Phillips Research Reports, 13, No. 1, 1 (1958)).

Table 463-VII

CALIBRATION OF VACUUM HIGH TEMPERATURE CALORIMETER  
 Calibration Constant, <sup>(1)</sup>  
 cal/mv

Voltage	Current, amps	Time, min	Total Heat, cal.	Rate of Heating, cal/min	Calibration Constant, <sup>(1)</sup> cal/mv	
					A	B
34.223	0.9358	5	2296.3	459.3	2548.6	2520.7
34.200	0.9362	20	9183.1	459.2	2569.4	2520.7
35.988	0.9866	20	10,183.4	509.2	2569.2	2517.5
64.242	1.7610	5	8111.5	1622.3	2548.4	2524.6
53.751	1.4769	20	22,767.8	1138.4	2571.5	2523.9
Average					2561.5 ± 0.4%	2521.5 ± 0.1%

Note: (1) Column A calculated with  $\Delta\theta$  from equation (1)

(2) Column B calculated with  $\Delta\theta$  from equation (1), but with 2k for cooling rate.

The method requires four contacts on the periphery of a thin slab of uniform thickness, but arbitrary shape. The actual location of the contacts around the periphery is immaterial. The resistivity is calculated from two sets of potential measurements and the sample thickness. The method will allow electrical resistivity measurements to be made on thermal diffusivity samples.

The high temperature furnace has been received.

Some of the radiation shields were damaged during shipment.

#### Thermal Diffusivity

The cooling water system for the Korad K-2 laser is now operating with a new pump and filter. A new flash lamp reflector has been installed. The energy output of the laser has not deteriorated with time since completion of these repairs.

A series of thermal diffusivity measurements on samples of five different materials (Armco Iron, Inconel 702, Alloy A-286, Tungsten, and Molybdenum), with each material represented by three different thickness samples, was started. These samples will be used as standards for assessing the accuracy and precision of the measurements. The initial measurements indicated a significant sensitivity of the results to laser beam alignment and to the beam energy distribution. The same indications were found with both ruby and Nd-doped glass laser rods. Beam alignment will become less of a problem when fixed mounts for many of the components are obtained. Drawings for the mounts are completed and fabrication is just starting. Methods of

providing a uniform beam energy distribution are being investigated.

The Centorr high temperature furnace and its power supply have been received. The furnace is presently being installed for a cold mock-up of the diffusivity system.

#### 8a. Mechanical Properties

(M. Tokar)

##### A. Hot Hardness

Hot hardness tests were conducted on Pu<sub>2</sub>C<sub>3</sub>, using the apparatus described in previous reports. Diamond pyramid hardness indentations were made with a 200 gram load at temperatures up to 1000°C in vacuum. Two Pu<sub>2</sub>C<sub>3</sub> samples, containing < 5 v/o PuC, were tested.

The hardness data at temperatures from 500-1000°C on Pu<sub>2</sub>C<sub>3</sub> and on a PuC sample previously tested are shown in Fig. 463-5. Each data point represents the mean value of several runs, where in each run, 3-5 readings were taken at each temperature. The extreme hardness values obtained at each temperature are also shown.

It is evident that Pu<sub>2</sub>C<sub>3</sub> is considerably harder than PuC at temperatures above 500°C. The data may, however, also be plotted as hardness versus fraction of the absolute melting point for each compound. In this case Pu<sub>2</sub>C<sub>3</sub> would still be harder than PuC at comparable melting point fractions, but the gap would be smaller. For example, at 0.5 T<sub>m</sub> PuC has a DPH of about 170 versus 200 for Pu<sub>2</sub>C<sub>3</sub>.

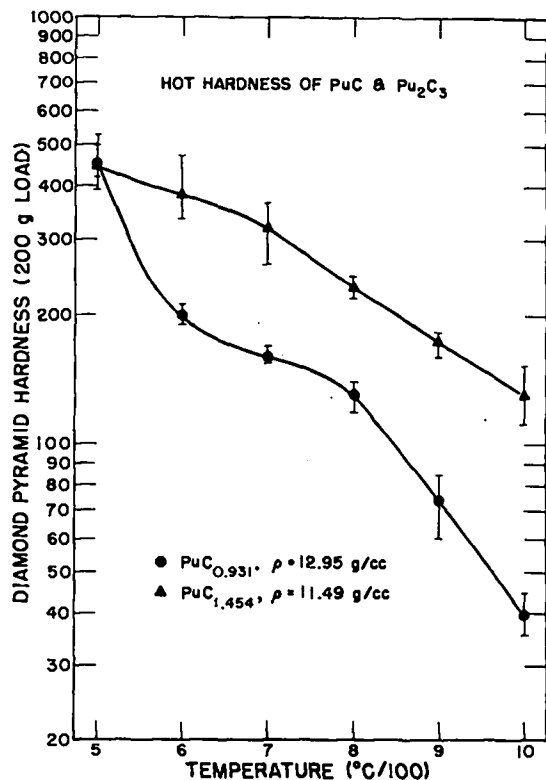


Figure 463-5

Modifications are being made to the hot hardness tester which will extend the maximum temperature capability to temperatures above 1000°C. These changes have been hindered by delays in the delivery of materials required in the fabrication of the furnace heating elements. The modifications should be completed, however, before the end of the current fiscal year.

#### B. Creep

The compressive creep of  $U_{0.8}Pu_{0.2}C$  has been measured at 1500°C and 2200 psi. The minimum creep rate was  $2.64 \times 10^{-3}$ /h. In comparison the creep rate of arc-cast hyperstoichiometric UC under these test conditions has been reported to be about  $8 \times 10^{-5}$ /h. The relatively high creep rate for the mixed carbide in the present study may be related to the low density (11.5 g/cm<sup>3</sup>) of the material. During the test at 1500°C and 2000 psi the  $U_{0.8}Pu_{0.2}C$  specimen was deformed 33.8% in 43 hours with an accompanying increase in density to 12.2 g/cm<sup>3</sup>. A major portion of this study is

concerned with the determination of the effects of microstructural variables such as porosity, grain size, etc., on creep rate.

Although at present specimen deformation is being measured with a micrometer, an optical extensometer is being set up which will allow the deformation to be measured in situ. Some delay was encountered due to a malfunction in the internal circuitry of the differential amplifier, but this has been rectified. The targeting has, however, been found to be extremely critical. In order to achieve a "lock-on", more light is required than is currently obtainable by reflection from the graphite susceptor to the vacuum chamber wall to the optical heads. The additional light will be obtained by introduction of two resistance-heated tungsten filaments into the vacuum chamber directly in the light path of the optical heads.

#### 8b. Special Problem

(J. L. Green and K. L. Walters)

#### B<sub>4</sub>C Structural Study

The summary of a recent attempt to characterize the powder diffraction patterns of various samples of B<sub>4</sub>C reported<sup>(6)</sup> analytical difficulties in the X-ray diffraction data could not be satisfactorily indexed in terms of the published structure<sup>(7,8)</sup> for B<sub>4</sub>C. Although the precise nature of the problem was not indicated, it was clear that the structure of B<sub>4</sub>C was considered to be in question. Similar difficulties have been reported by other investigators.<sup>(9)</sup> In other instances, apparently no attempt was made to index the back-reflection pattern even though the position of particular lines as functions of composition were reported.<sup>(10)</sup> No indexed, high angle line lists for experimentally observed powder patterns have been reported in the literature. This apparent indexing difficulty may account in part for the fact that no high precision lattice parameters have been reported. Uncertainties regarding the basic structure must be eliminated before crystallographic data may be effectively used for properties studies or in routine materials characterizations. In order to demonstrate that observed powder patterns are consistent with a particular structure, it is necessary to show first that

observed line positions are proper and second that observed reflection intensities are those defined by the structural model. The first requirement shows that the reported size and shape of the crystal lattice is correct while the second shows that the atomic positions defined by the structure description are consistent with observations. Showing that the powder pattern defined by the published structure is consistent with observation does not necessarily prove that the structure is correct; however, it would eliminate the basis for the challenges regarding the symmetry of the structure that have been presented in the literature.

Neutron diffraction techniques have never been applied to the study of  $B_4C$ . It is possible that such data would be useful in certain areas of the problem. Neutron diffraction patterns characteristically have low resolution; therefore, studies of precise line positions are best carried out using X-ray techniques. The area in which neutron data would be most useful is the study of reflection intensities. The accurate measurement of X-ray reflection intensities is a difficult problem. However, neutron intensities can be measured with good accuracy under appropriate experimental conditions. The advantages of neutron diffraction result from the facts that (1) accurate absorption corrections are possible, and (2) no uncertainties are introduced by the use of form factors since nuclear scattering factors are independent of the diffraction angle. The primary experimental difficulties will be associated with the absorption effects. Due to the fortuitous near equality of the scattering amplitudes of  $^{12}C$  and  $^{11}B$ , it will be necessary to use material containing a substantial amount of  $^{10}B$  to make it possible to differentiate between C and B positions in the structure. The absorption coefficients for thermal neutrons will be large; therefore, thin targets will be required. The major problem will be the preparation of targets that are sufficiently thin and uniform but still containing enough material to produce a satisfactory diffraction pattern.

The following is being done to evaluate the feasibility of such studies:

1. Test the consistency of line positions with the published structure using standard X-ray powder techniques. This must be done before meaningful intensity studies may be made.
2. Develop techniques for the preparation of thin neutron diffraction targets of  $B_4C$  and test the consistency of observed intensities with those defined by the published structure.

If these investigations indicate that the structure is nominally correct, the technique could further be applied to studying the structural effects of changes in the B/C ratio within the stoichiometry range of " $B_1C$ ". A study of the mechanisms by which excess boron and/or carbon are accommodated by the structure would be of considerable interest. The method could also prove useful in the study of the structural effects of radiation damage.

The first item of the proposed investigation has been essentially completed. Debye-Scherrer powder diffraction patterns were obtained on several samples of commercial grade, carbon-rich  $B_4C$  and analyzed. The patterns from the various samples appeared to be essentially identical. The analytical data for this material is shown in Table 463-VIII.

Table 463-VIII  
 $B_4C$  ANALYTICAL DATA <sup>(1)</sup>

Pycnometric Density	2.52 gm/cm <sup>3</sup>		
Bulk Density	0.57 gm/cm <sup>3</sup>		
Tap Density	0.92 gm/cm <sup>3</sup>		
B	75.9%		
C	21.8%		
O <sub>2</sub>	0.76%		
N <sub>2</sub>	320		
Li	< 10	Ni	< 30
Be	< 3	Cu	30
Na	< 100	Zn	< 100
Mg	< 3	Sr	< 30
Al	30	Zr	< 100
Si	300	Nb	< 300
K	< 300	Ag	< 3
Ca	< 30	Cd	< 30
Ti	< 300	Sn	< 30
V	< 100	Ba	< 30
Cr	< 30	W	< 300
Mn	10	Pb	20
Fe	500	Bi	< 10
Co	< 30		

(See Note on following page)

Note: (1) Kawecki Chemical Co. B<sub>4</sub>C (Lot No. 292-83). Chemical analyses reported as ppm by weight unless otherwise indicated.

The powder patterns were taken using a 114.6 mm diameter Norelco Debye-Scherrer camera. Copper radiation was used; however, a  $6 \times 10^{-4}$  in. thick internal Ni filter was used to eliminate the K $\beta$  component. In order to enhance weak lines a large capillary (0.5 mm diameter) and relatively long exposures were used. This allowed most of the lines in the pattern to be recorded. However, it resulted in severe overexposure of several of the low angle lines. The unambiguous back-reflection lines were used to compute least squares fitted lattice parameters. The fit appears to be good, with all deviations reasonably accounted for by random errors in measurement. The fit was made using a Nelson-Reiley extrapolation function. Because the program used in the fitting was not directly applicable to a rhombohedral lattice, the fit was done in terms of the alternate hexagonal unit cell. The results of this fit are

$$a_o = 5.6016 \pm 0.0010 \text{ \AA}$$
$$c_o = 12.072 \pm 0.003 \text{ \AA}$$

where the error limits are 95% confidence intervals with respect to internal consistency. These correspond to a rhombohedral unit cell with

$$a_o = 5.1625 \text{ \AA}$$
$$\alpha = 65.65 \text{ deg.}$$

The only lattice parameters available in the literature for comparable material are those reported by Allen<sup>(11)</sup> for B<sub>4</sub>-C. He reported  $a_o$  to be 5.61 Å and  $c_o$  to be 12.07 Å for the hexagonal unit cell as calculated from low angle data. Agreement is satisfactory. Elliot<sup>(10)</sup> presented the results of diffraction measurements on B<sub>4</sub>C as a function of composition by reporting the angular position of what he termed "the strong back-reflection of B<sub>4</sub>C". The strongest high angle line in the B<sub>4</sub>C pattern is the  $\overline{511} - 333_{\alpha_1}$  which was observed in the present study of  $152.77^\circ 2\theta$ . Elliot reported his line at  $152.84^\circ 2\theta$  for carbon saturated B<sub>4</sub>C. The two line positions are identical to within errors in measurement.

The graphite lattice parameters estimated from

these data are

$$a_o = 2.51 \text{ \AA}$$
$$c_o = 6.66 \text{ \AA}$$

Although these parameters are very approximate, they imply rather large boron solution in the graphite.<sup>(12)</sup>

Two minor anomalies were observed in the pattern. The first has to do with the line occurring at  $48.90^\circ 2\theta$ . This reflection was indexed as the B<sub>4</sub>C 220; however, the observed intensity appears somewhat larger than would be expected from calculated intensities. The reason for this discrepancy is not known, but it could be due to minor inaccuracies in the positional parameters used in the calculations. The second problem is in regard to the weak line observed at  $151.03^\circ 2\theta$ . It has not been possible to identify this reflection. It does not appear to belong to the B<sub>4</sub>C pattern. It may be due to the graphite phase. Except for these items, the observed pattern appears to be satisfactorily consistent with the published structure with respect to both line position and estimated intensity. It is concluded, therefore, that X-ray powder data for carbon saturated B<sub>4</sub>C present no basis for challenging the published structure. It should be noted, however, that the intensity considerations presented above are not sufficiently sensitive to constitute a thorough test of all the details of the structure description to which powder data can be applied, e.g., positional parameters, etc. Evaluation studies on the applicability of neutron diffraction techniques to the problem are in progress.

#### 9. New Facilities (A. L. Gonzales)

##### New Mass Spectrometer - Room 601

An enclosure for this apparatus has been designed. A purchase order has been written requesting bids for fabrication.

##### Hot Hardness - Room 604

All the new pieces except for the heating element are on hand to convert this unit for work at temperatures of  $1400^\circ \text{C}$ . A new B<sub>4</sub>C indenter has been fabricated by the Shops Dept. and appears to be acceptable. An order has been written for the installation of new services which are to be required for this facility.

### Cooling Water Modifications - Building 150

An engineering study has been made by ENG-2 to increase the cooling water capacity throughout Building 150. One of the primary benefits to be gained will be that this area will now be independent from the rest of the plant, eliminating present water outages, low pressure and inadequate chilled water.

A study is also being made with regard to the negative pressure chilled circulating water. It appears that we have exceeded the capacity of the present system in that the negative water, which is cooled by heat exchanges, is entering and leaving the system at such a fast rate that the water is not able to be cooled fast enough. The addition of a larger heat exchanger should solve this problem.

#### IV. ANALYTICAL CHEMISTRY

##### 1. Determination of O<sub>2</sub> in Refractory Oxides, Carbides, and Nitrides

(M. E. Smith and J. E. Wilson)

Modifications to improve the method for measuring O<sub>2</sub> in ceramic Pu fuel materials are being investigated because of the great effect of this element on the properties of refractory oxides, carbides, and nitrides. One promising modification is the use of a microwave-excited, emissive detector system to measure the O<sub>2</sub> evolved as CO as the sample is inductively heated to 2000°C in a C crucible. Microwave excitation of the CO causes a glow discharge that is monitored photometrically, and the O<sub>2</sub> concentration is calculated from the time-integrated signal from the photometer. Repeated analyses of several refractory oxides used as standard materials for oxide fuels, show that the precision (1σ) and the bias are 2 relative percent or less (Table 463-IX). The calculations are based on a standard curve prepared from data obtained for various amounts of U<sub>3</sub>O<sub>8</sub>. Data are being obtained to extend the range of the calibration curve and to determine if calibration for each specific oxide is necessary for better precision and accuracy.

A second modification being investigated is substitution of impulse heating for induction heating of the sample. For this type of heating, the sample is placed in a covered C capsule, and a large direct current of

Table 463-IX

#### DETERMINATIONS OF O<sub>2</sub> IN REFRACTORY OXIDES

Oxide	Calculated O <sub>2</sub> Content, %	No. of Determinations	Av. O <sub>2</sub> Found, %	Rel. Std. Dev., %
U <sub>3</sub> O <sub>8</sub>	15.18	5	15.12	0.8
ZrO <sub>2</sub>	25.73	5	25.81	1.6
ThO <sub>2</sub>	12.16	5	12.19	0.9
Nb <sub>2</sub> O <sub>5</sub>	30.10	5	30.18	1.1
Ta <sub>2</sub> O <sub>5</sub>	18.10	5	17.77	0.6

short duration heats the capsule to about 3000° in 1 to 2 sec. The O<sub>2</sub> in the sample is evolved as CO which is trapped on SiO<sub>2</sub> gel cooled in liquid N<sub>2</sub> and then measured on a gas chromatograph.

Initial tests by analyzing prepared U<sub>3</sub>O<sub>8</sub>-TaC mixtures, each weighing about 5 mg., showed that the relative standard deviation of the method was about 10 percent. Air trapped in the capsule during loading of the sample was found to contribute significantly to the high reagent blanks and to affect the precision of the method adversely. The heater and sample-loading systems were redesigned to make the apparatus more compact, and a small dry box containing a He atmosphere was attached for loading the samples. Testing of the modified equipment was started to determine if the apparatus blank was reduced.

#### V. REFERENCES

1. G. M. Campbell, "Thermodynamic Properties of Plutonium Nitride by Galvanostatic Potential Determination," *J. Phys. Chem.* **73**, 350 (1969).
2. R. A. Kent, "Mass Spectrometric Studies of Plutonium Compounds at High Temperatures. V. The Plutonium-Carbon System", presented at the International Conference on Mass Spectroscopy, Kyoto, Japan, September 8-12, 1969.
3. R. A. Kent, *High Temperature Science* **1**, 169 (1969).
4. M. H. Rand, "A Thermochemical Assessment of the Plutonium-Carbon System," presented at IAEA, Vienna, Sept. 1968.
5. JANAF Thermochemical Tables, the Dow Chemical Co., Midland, Mich. (1965).
6. U. S. A. E. C. Report, ORNL-4480, pp 130 (1969).
7. H. K. Clark and J. L. Hoard, *J. Am. Chem. Soc.* **65**, 2115-2119 (1943).
8. G. Zdanov and N. Sevastyanov, *Compt. Rend. (Doklady) Acad. Sci. U. S. S. R.* **32**, 432 (1941).

9. R. Kranz, *Hamburger Beitr. Agnew. Mineral. Kristallphy. Petrogen.* 2, 99-115 (1959).
10. U. S. A. E. C. Report ARF-2200-12 (1961).
11. R. D. Allen, *J. Am. Chem. Soc.* 75, 3582 (1953).
12. C. E. Lowell, *J. Am. Ceram. Soc.* 50, 142 (1966).

PROJECT 464

STUDIES OF Na-BONDED (U,Pu)C LMFBR FUELS

Person in Charge: D. B. Hall  
Principal Investigator: J. C. Clifford

Funding for this program will not continue beyond the end of FY-1970. A final report on the work (and on the also discontinued Fast Reactor Metal Fuels Program) will be included in the Fourth Annual Report on the Advanced Plutonium Fuels Program, which will be issued at the end of the current fiscal year. Additional topical reports may be prepared as part of the phaseout activities during the balance of FY-1970.

PROJECT 465

REACTOR PHYSICS

Person in Charge: D. B. Hall  
Principal Investigator: G. H. Best

---

I. INTRODUCTION

Basic to the evaluation of various fast breeder concepts and proposals are the analytical techniques and physical data used in the analyses. Valid comparisons between different concepts and proposals depend on minimization of differences in results due to methods of analyses. To this end, the Los Alamos Scientific Laboratory is cooperating with other AEC laboratories and contractors in the development of evaluated cross-section data and associated processing codes. In addition, the Laboratory is working on the development and maintenance of digital computer programs pertinent to the nuclear analysis of fast breeder concepts. The Laboratory is also adapting, modifying, and evaluating modular programming systems for comprehensive nuclear analysis. Finally, the Laboratory is evaluating the performance characteristics of various fast breeder reactor concepts.

II. CROSS-SECTION PROCUREMENT, EVALUATION, AND TESTING (M. E. Battat, D. J. Dudziak, R. J. LaBauve, R. E. Seamon)

A. General

Accurate predictions of reactor design parameters, such as critical mass, material worths, and spectral response, require the development and maintenance of up-to-date basic microscopic nuclear data files. To meet this end, a national cooperative program is in progress to prepare an evaluated nuclear data file (ENDF/B). The large amount of experimental data which is becoming available, together with theoretical data, makes the maintenance of ENDF/B a continuing task. In addition, a large effort is needed in evaluating and testing the microscopic data prior to use in reactor calculations.

B. Codes

1. MC<sup>2</sup>. In response to a request from the Reactor Physics Division at Argonne National Laboratory, recommendations were submitted for additions to and improvements in the MC<sup>2</sup> code. Also, the code and the current ENDF/B library tape were sent to Kirtland AFB.

2. LAPH. Final testing of the LAPH code has been successfully completed, and the code has been edited using TIDY and INDEX. The report which documents the LAPH code has been completed and is now in press. Several modifications were made in the tape handling parts of the code to reduce the long execution time when there are several materials on the ENDF/B data tape, as is the case with the sample problem. The central processor time was reduced by about a factor of two, as was the peripheral processor time.

3. PHOXE. The "physics" checking code for photon production data in the ENDF/B format, PHOX, has been extensively revised and extended and is now designated PHOXE. It has undergone final debugging and has been submitted to the Radiation Shielding Information Center (RSIC) Computer Code Collection. Prior to submission, it was processed by the codes TIDY and INDEX, in order to improve its documentation and adaptability. Changes and additions that have been made to the code since its previous documentation<sup>1</sup> include:

a. Adaptation to the CDC-6600 FORTRAN compiler from the Burroughs B5500 FORTRAN compiler. The principal changes involved clearing of memory (initializing), which is done automatically on the B5500. Also, on the B5500, the memory is cleared for each subroutine after each exit from the subroutine, so all variables which need to be saved

must be in COMMON. This use of COMMON was retained to facilitate adaptation of PHOXE to machines with compiler features similar to the B5500. Other minor adaptations included incorporation of end-of-file checks, expanded COMMENT cards, and improved format of output flags.

b. Subroutine arguments which are integers were redefined where they appeared as floating-point variables, because the CDC 6600 will float the integer where this occurs, as opposed to the B5500.

c. The ENDF/B tape search routine was revised to read tape labels with Hollerith information, which present ENDF/B tapes have. The TPID card formerly required a LIST card format.

d. The ES-EG pair routine was completely rewritten (1) to check that each ES-EG pair in File 14 appears somewhere in File 15, (2) to flag ES-EG pairs which appear in File 15 under a different MT (reaction type) number, and (3) to flag all ES-EG pairs in File 15 which do not appear in File 14, i.e., have no angular distribution given. Isotropic distributions in File 14 are now paired with photons in File 15 for the corresponding number.

e. Many Hollerith formats that are written upon detection of an error (or possible error) were revised to be more explicit and grammatical. Energy units were standardized as electron-volts.

f. A  $10^{-5}$  error criterion was applied to the checking of the first tabulated energy in a File 3 TAB1 record against a theoretical threshold computed from the Q value. The same criterion was applied to the incident-neutron energies in File 14 and File 15 TAB1 records. Q values are now checked for reasonableness, based upon the reaction type (e.g.,  $Q < 0.0$  for inelastic scattering reactions). Photon energies are checked and flagged if less than  $10^5$  eV, which serves to detect erroneous entries of energies in units of MeV. For polyisotropic materials,  $Q = 0.0$  is often entered in the ENDF/B file for radiative capture (MT=102), so a Q value of  $8 \times 10^6$  eV is assumed by PHOXE for purposes of checking reaction energetics (total photon energy release vs Q plus incident center-of-mass neutron energy). Also, the total photon energy released is printed for informational purposes, even if it does not exceed the theoretical maximum.

This is especially useful for detecting missing photon energy in, for example, radiative capture.

g. The subsections in File 14 and 15 are now examined to verify that the photon energies appear in decreasing magnitude within each section, and that the continuum (if present) appears last. Also, if more than one continuum subsection is present, an error comment is printed.

The PHOXE code was debugged by processing sodium, magnesium, silicon, chlorine, potassium, and calcium data. Special emphasis was placed on the silicon and calcium data because these data are being provided for some LASL test calculations of photon production in concrete.

### C. Data Testing

Proposed re-evaluations of the ENDF/B data for  $^{235}\text{U}$ ,  $^{238}\text{U}$ ,  $^{239}\text{Pu}$ ,  $^{240}\text{Pu}$ ,  $^{241}\text{Pu}$ , iron, chromium, niobium, molybdenum, and  $^{232}\text{Th}$  were distributed during this report period by the National Nuclear Cross-Section Center at Brookhaven for testing by the members of the Cross-Section Evaluation Working Group. These data have been processed in order to obtain cross-section sets from MC<sup>2</sup> for use in the calculation of fast critical assemblies JEZEBEL and GODIVA. The re-evaluated data include several options which are allowed in the ENDF/B specifications but which are not implemented in the data processing codes. These format changes have necessitated revisions in the standard ENDF/B processing codes CHECKER, DAMMET, ETOE, MERMC2, and MC<sup>2</sup>. Revised versions of DAMMET and CHECKER were provided by BNL. Several changes in the data, as received, had to be made before they could be processed.

In connection with changes in the data format, two codes called MAKE4 and PUNCH were written. For materials iron,  $^{239}\text{Pu}$ ,  $^{240}\text{Pu}$ , and  $^{241}\text{Pu}$ , there is no total inelastic cross section (MT=4) given in File 3, but only the cross sections for discrete levels ( $5 \leq \text{MT} \leq 14$ ,  $51 \leq \text{MT} \leq 80$ ) and the continuum (MT=15). The code MAKE4 combines the cross sections and calculates the probability distributions, viz.,

$$\sigma_{\text{MT}=4}(E) = \sum_i \sigma_{\text{MT}=i}(E) ,$$

and

$$P_i(E) = \frac{\sigma_{\text{MT}=i}(E)}{\sigma_{\text{MT}=4}(E)} ,$$

where

$$5 \leq i < 15, 51 \leq i \leq 80$$

Program PUNCH was written to prepare cards for ETOE from File 2 unresolved resonance data given under the LRU=2, LRF=2 option as is the case for materials  $^{235}\text{U}$ ,  $^{238}\text{U}$ ,  $^{239}\text{Pu}$ , and  $^{241}\text{Pu}$ . The two codes have been sent to the NNCSC.

Several additional changes in the re-evaluated data for materials  $^{235}\text{U}$ ,  $^{238}\text{U}$ ,  $^{239}\text{Pu}$ ,  $^{240}\text{Pu}$ , and  $^{241}\text{Pu}$  were received during the first week of March. These changes were made, and a binary input tape for MC<sup>2</sup> was prepared. Copies of this tape were supplied to all CDC-6600 users in CSEWG.

Successful MC<sup>2</sup> runs have been made with all re-evaluated materials, except molybdenum and niobium. Additional changes in MC<sup>2</sup> will be required before these data can be processed. Preliminary results obtained for JEZEBEL and GODIVA are given in Tables 465-I and 465-II. These tables were distributed at the CSEWG meeting at Brookhaven on March 24 and 25.

### III. REACTOR ANALYSIS METHODS AND CONCEPT EVALUATIONS

#### A. General

A continuing task in fast reactor analysis and evaluation is the improvement of computer programs and the development of new computational methods. In addition to new methods, advances are constantly being made in computer technology which make possible the extension of existing calculational techniques.

#### B. Preparation and Maintenance of Code Packages

1. Two-Dimensional Perturbation Code DAC2 (G. C. Hopkins). The two-dimensional perturbation code DAC2 has been written and compiled. The code presently is being checked out with a test problem.

The code was built up from parts of two other codes: the two-dimensional  $S_n$  transport code<sup>2</sup> 2DF, and the one-dimensional perturbation code DAC1. First, the input and data preparation subroutines from 2DF were set up. Then, a subroutine SORT was added to reorder and combine the angular fluxes put

TABLE 465-I

\*\*PRELIMINARY COMPARISONS OF REEVALUATED ENDF/B DATA AND EXPERIMENT\*\*  
\*\*FAST REACTOR BENCHMARK PROBLEM NO. 1 - - J E Z E B E L \*\*  
\*\*LOS ALAMOS SCIENTIFIC LABORATORY 17 MARCH 1970\*\*

- I. SYSTEM DESCRIPTION---AS GIVEN IN MEMORANDUM FROM H. ALTER TO PHASE II DATA TESTING PARTICIPANTS, DATED 26 JANUARY 1970. GALLIUM NOT INCLUDED.
- II. MODEL DESCRIPTION---DTF-IV TRANSPORT THEORY. S-16. STANDARD 26 HALF-LFTHARGY-WIDTH GROUP STRUCTURE. SPATIAL MESH--10 INTERVALS BETWEEN R = 0.0 AND R = 0.7268 CM, 15 BETWEEN R = 0.7268 AND 6.385 CM. STATIC K-EFF CALCULATION WITH 1.0E-05 CONVERGENCE CRITERION.
- III. DATA SOURCE DESCRIPTION---REEVALUATED ENDF/B DATA. DATA PROCESSED USING VERSIONS OF ETOE AND MC\*\*2 MODIFIED TO HANDLE FORMAT CHANGES. P-1 FUNDAMENTAL MODE CALCULATION (IOPT=1) WITH ALL-FINE-GROUP OPTION.
- IV. COMPUTATIONAL RESULTS---MULTIPLICATION FACTOR MEASURED VALUES TAKEN FROM MEMORANDUM DATED 21 FEBRUARY 1969 BY W.G. DAVEY AND A.L. HESS TO MEMBERS OF THE CSEWG.  
K-EFF (ISOTROPIC TRANSPORT) = 0.98846  
CORRECTIONS--GALLIUM EFFECT = +0.0035  
S-INFINITY MINUS S-16 = -0.00093  
P-3 MINUS ISOTROPIC TRANSPORT = -0.002  
K-EFF CORRECTED = 0.98903  
= 1.000 MEASURED (+ OR - 0.003)
- V. COMPUTATIONAL RESULTS---CENTRAL FISSION RATIOS MEASURED VALUES TAKEN FROM MEMORANDUM DATED 21 FEBRUARY 1969 BY W.G. DAVEY AND A.L. HESS TO MEMBERS OF THE CSEWG.  
(PU-239/U-235) = 1.37  
= 1.49 MEASURED (+ OR - 0.03)  
(U-238/U-235) = 0.181  
= 0.205 MEASURED (+ OR - 0.008)

TABLE 465-II

**\*\*PRELIMINARY COMPARISONS OF REEVALUATED ENDF/B DATA AND EXPERIMENT\*\***  
**\*\*FAST REACTOR BENCHMARK PROBLEM NO. 5 - - G O D I V A \*\***  
**\*\*LOS ALAMOS SCIENTIFIC LABORATORY 17 MARCH 1970\*\***

- I. SYSTEM DESCRIPTION--AS GIVEN IN MEMORANDUM FROM H. ALTER TO PHASE II DATA TESTING PARTICIPANTS, DATED 26 JANUARY 1970.
- II. MODEL DESCRIPTION---DTF-IV TRANSPORT THEORY. S-16. STANDARD 26 HALF-LENGTH-WIDTH GROUP STRUCTURE. SPATIAL MESH--10 INTERVALS BETWEEN R = 0.0 AND R = 0.7268 CM, 20 BETWEEN R = 0.7268 AND 8.741 CM. STATIC K-EFF CALCULATION WITH 1.0E-05 CONVERGENCE CRITERION.
- III. DATA SOURCE DESCRIPTION---REEVALUATED ENDF/B DATA. DATA PROCESSED USING VERSIONS OF ETOE AND MC\*\*2 MODIFIED TO HANDLE FORMAT CHANGES. P-1 FUNDAMENTAL MODE CALCULATION (IOPT=1) WITH ALL-FINE-GROUP OPTION.
- IV. COMPUTATIONAL RESULTS---MULTIPLICATION FACTOR  
 MEASURED VALUES TAKEN FROM MEMORANDUM DATED 21 FEBRUARY 1969 BY W.G. DAVEY AND A.L. HESS TO MEMBERS OF THE CSEWG.  
 K-FFF (ISOTROPIC TRANSPORT) = 1.00219  
 CORRECTIONS--S-INFINITY MINUS S-16 = -0.00093  
 P-3 MINUS ISOTROPIC TRANSPORT = -0.002  
 K-FFF CORRECTED = 0.99926  
 = 1.000            MEASURED            (+ OR - 0.003)
- V. COMPUTATIONAL RESULTS---CENTRAL FISSION AND CAPTURE RATIOS  
 MEASURED VALUES TAKEN FROM MEMORANDUM DATED 21 FEBRUARY 1969 BY W.G. DAVEY AND A.L. HESS TO MEMBERS OF THE CSEWG.  
 ( U-238 F)/(U-235 F) = 0.155  
 = 0.156    MEASURED            (+ OR - 0.005)  
 (PU-239 F)/(U-235 F) = 1.36  
 = 1.42    MEASURED            (+ OR - 0.02)  
 ( U-238 C)/(U-238 F) = 0.553  
 = 0.47    MEASURED            (+ OR - 0.02)

out by a revised version of 2DF. Finally, the computational subroutines of DAC1 were added and modified for two dimensions.

2. Adaptation of DAC to Standard Interfaces  
 (B. M. Carmichael and J. C. Vigil). Revised standard interfaces between the codes ETOX-LDX (cross-section processing), ANISN (one-dimensional  $S_n$ ), DOT (two-dimensional  $S_n$ ), 2DB (two-dimensional diffusion), and DAC perturbation were recently established by the Committee on Computer Code Coordination. DAC is being revised locally to calculate reactivity perturbations from standard interface data supplied by diffusion or  $S_n$  codes in one, two, or three dimensions.

The standard interfaces, or files, needed in DAC are:

1. ADMNSTR (administration and control file containing dimensions and option control data).
2. GEO DIST (geometry and material distributions).
3. SN CONS (SN constants).

4. INTQUANT (integral quantities such as zone volumes and zone-averaged fluxes).
5. MIX DATA (mixture data).
6. MULTIGRP (multigroup cross-section file).
7. GRP FLXS (group fluxes).

Both unperturbed and perturbed versions of MULTIGRP and regular and adjoint versions of GRP FLXS are required by the perturbation codes.

To make it possible to use generalized reading routines on the standard files, all files are first preprocessed to place Hollerith, fixed-point, and floating-point data in separate records containing no more than one vector per record. Next, the flags, IREAD(I), are read from cards for each File I.

- IREAD(I) = 1 denotes all File I data to be read from cards,  
 IREAD(I) = 2 denotes all File I data to be read from the standard file, and  
 IREAD(I) = 3 signals File I data to be read from both cards and a file.

If Option 3 is exercised, then additional flags IRD(I,J) are read from cards to signify that the data of type J in File I are to be read from cards (IRD(I,J)=0) or are to be read from an existing file (IRD(I,J)=1). If any data are to be read from cards, then both an old and new version of the given file will exist. The new version will contain the updated data read from cards.

The limited amount of Hollerith information contained in the files is read by special read statements provided for each Hollerith record. Fixed-point and floating-point data are read, respectively, by the generalized read subroutines, REAFX and REAREL. The argument list in these routines contains ARRAY, NWDS, IFG, (HOLL(K),K=1,6), IRD(I,J), and IPRIN. The vector ARRAY containing NWDS words is read by the subroutine. The array IFG contains these five items:

IFG(1) specifies the input file for card data,  
 IFG(2) specifies the output print file,  
 IFG(3) identifies the old standard file,  
 IFG(4) identifies the new standard file, and  
 IFG(5) = IREAD(I).

ARRAY and its Hollerith description contained in (HOLL(K),K=1,6) are printed only if IPRIN = 1.

DAC uses 21 files; nine of the files are input standard files, and allowance is made for nine output or modified files. In addition, three scratch files are required. To avoid allocating the excessive core memory space (21,525 words) for buffering all 21 files simultaneously, a COMPASS subroutine obtained from Knolls Atomic Power Laboratory (KAPL) is used which permits the reassignment of buffer areas during execution. By using this COMPASS subroutine, the number of buffers required is reduced to seven.

The revisions to DAC are completed, and test problems are being run prior to distributing the code to the Committee for tests on other computers.

3. 3DDT Code (J. C. Vigil). A sample three-dimensional problem was received from Battelle Northwest Laboratory to be run with the 3DDT code for comparison with the 3DB code.<sup>3</sup> The sample problem is a two-group, two-region, one-step burnup calculation in X-Y-Z geometry. The reactor consists of a cubical core region, 80 cm on a side, surrounded on all sides by a blanket region, 30 cm thick.

Thus, the reactor is a cube, 140 cm on a side. Initial compositions of the core and blanket regions are given in Table 465-III.

TABLE 465-III

INITIAL COMPOSITIONS OF CORE AND BLANKET ZONES

Material	Atom Density in Units of $10^{24}$	
	Zone 1 (core)	Zone 2 (blanket)
$^{238}\text{U}$	0.0080	0.0400
$^{239}\text{Pu}$	0.0016	0.0
$^{240}\text{Pu}$	0.0001	0.0
$^{241}\text{Pu}$	0.0	0.0
Fission products	0.0	0.0
C	0.0200	0.0
Na	0.0060	0.0
Fe	0.0130	0.0062

Because of symmetry, only one octant of the reactor was represented in the calculational model, which contained ten intervals in each dimension. A reflective boundary condition was applied to the interior boundaries of the octant, and a vacuum boundary condition was applied to the exterior boundaries.

The initial  $k_{\text{eff}}$  calculation was followed by a burnup interval of 50 days with the reactor at 800 MWt total power. Following the burnup interval, a final  $k_{\text{eff}}$  was computed for the new material compositions resulting from fuel depletion, breeding, and fission-product buildup.

Results obtained with 3DDT on a CDC-6600 computer are shown in Table 465-IV, along with results

TABLE 465-IV

SUMMARY OF 3DDT AND 3DB RESULTS

	Initial System	
	3DB	3DDT
Converged lambda	0.999998	0.999996
Multiplication factor	1.02172	1.02172
Total		
Flux at K=J=I=1	$2.02526 \times 10^{16}$	$2.02524 \times 10^{16}$
Flux at K=1, J=I=10	$2.84968 \times 10^{13}$	$2.84935 \times 10^{13}$
Outer iterations	10	10
Z iterations	84	84
X-Y iterations	3638	1679
Running time (min)	2.13	0.35
	Depleted System	
Converged lambda	0.999991	0.999990
Multiplication factor	0.99959	0.99961
Breeding ratio	1.6764	1.6765
Total		
Outer iterations	6	9
Z iterations	51	37
X-Y iterations	2022	1669
Running time (min)	1.28	0.34

obtained by Battelle with the 3DB code on a UNIVAC-1108 computer. As seen in Table 465-IV, results obtained with 3DDT and 3DB agree very well. However, the running time with 3DDT was about five times shorter than with 3DB. This is due to the differences in the CDC and UNIVAC computing systems, and the fact that 3DDT used fewer X-Y iterations.

A document that describes the 3DDT code has been written and will be issued as a Los Alamos Scientific Laboratory report.

4. Burnup-Refueling Code PHENIX (T. J. Hiron). The burnup-refueling code<sup>4,5</sup> PHENIX has been modified so that the complete fuel-cycle history, i.e., the entire series of burnup intervals, can be calculated in one run. Data dump capabilities are also provided so that the problem can be restarted after any number of burnup intervals. This multi-interval modification requires only two additional input control words but reduces the maximum allowable storage in the A Common Block from 30,000<sub>10</sub> to approximately 27,000<sub>10</sub> words. Several test problems have been run to check out the multi-burnup interval option.

C. Fast Reactor Design Analysis

1. Calculational Models (T. J. Hiron). The paper, "Calculational Models for Fast Reactor Fuel-Cycle Analysis," by Thomas J. Hiron and R. Douglas O'Dell has been revised and accepted for publication in Nuclear Applications and Technology. It will appear in the July issue.

2. Review of Synthesis Methods for Fast Reactor Analysis (R. E. Alcouffe). A topical review of the status of synthesis methods for fast reactor analysis has been initiated. Thus far, a literature search has been compiled and evaluated. The most pertinent topics applicable to this review are in the areas of (1) transport flux synthesis, (2) space-energy synthesis, and (3) space-energy-time synthesis for transient and fuel-cycle analysis.

D. Synthesis of Static Multigroup Transport Flux (R. E. Alcouffe). The technique described in Ref. 6 for employing the two-dimensional transport estimate of the flux from one-dimensional multigroup transport calculations has been applied to a fast reactor cell problem. This calculation will be used to estimate the heterogeneity effect for generating cell-averaged cross sections.

The technique itself utilizes information generated from one-dimensional transport calculations across a cell to form a two-dimensional estimate of the leakage. This leakage information is furnished by a two-dimensional diffusion code that computes the appropriate two-dimensional flux. To efficiently carry out this procedure on a computer, the DATATRAN system<sup>7</sup> has been employed. This system allows manipulation or linkage of existing codes by a FORTRAN program. The data computed or used by the separate codes can also be manipulated in the same way as FORTRAN variables and saved on a cataloged library tape for possible later use.

The system used to synthesize the two-dimensional transport flux consists of the DTF-IV code,<sup>8</sup> which does the one-dimensional transport calculation and the 2DB code,<sup>9</sup> which performs the two-dimensional diffusion theory calculation. An experimental intermediate code was written to compute the leakage coefficients. This system was used to calculate the flux in the cell shown in Fig. 465-1. Region I is a beryllium oxide rod, Regions II and IV are <sup>238</sup>U rods, where the total cross section of <sup>238</sup>U is taken to be 1000 b to simulate a resonance, and Region III is sodium. Three one-group calculations were performed to compare the effects of different approximations to compute the flux; the zone-integrated flux is shown in Table 465-V. These three computations are, respectively, two-dimensional transport (TWOTRAN-XY), two-dimensional synthesis

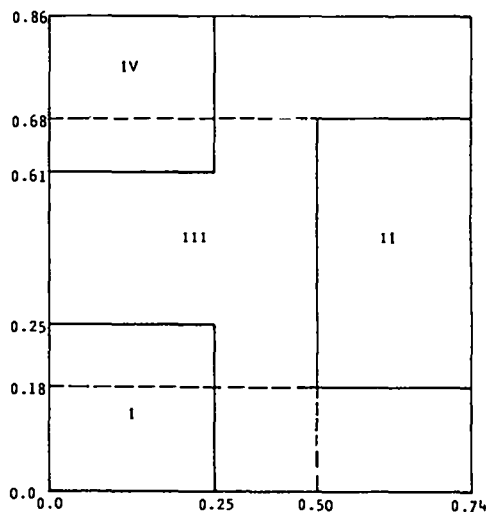


Fig. 465-1. Fast reactor calculational cell model.

TABLE 465-V  
 AVERAGED CELL FLUXES FROM  
 APPROXIMATE TWO-DIMENSIONAL CALCULATIONS

Zone	Reference Fluxes TWOTRAN-XY	% Deviation from Reference	
		DTF + 2DB	2DB
I	1.424	- 3.4	+88.3
II	0.1479	+25.5	-99.1
III	1.332	- 1.0	- 9.5
IV	0.1557	+25.5	-99.1
CDC 6600 CP time (sec)	165	36	31

(DTF+2DB), and two-dimensional diffusion (2DB). As can be seen from the table, there is a large error in the fuel regions when the results of the latter two approximate calculations are compared to the reference TWOTRAN-XY calculation. The reason for this is currently being investigated to correct the technique.

E. Space Collapsing for Fast Breeder Fuel-Cycle Analysis (R. E. Alcouffe and T. J. Hiron). A method previously has been described which makes possible the accurate analysis of the fuel-cycle history of a large fast breeder.<sup>10</sup> In brief, a static reference calculation of the system (trial solution) is used to reduce the number of mesh points in space and energy needed to perform an accurate time-dependent analysis of the system. A limit condition is established which states that, when reduced equations are found by the correct use of a trial solution, the reduced equations are exact, independent of the number and distribution of mesh points. It can be implied from this condition that, when the trial solution is not exact, mesh points need be concentrated only in the regions where the expected solution differs greatly from the trial solution. This effect is made clear in the example presented below. The technique was used previously to solve the problem of energy collapse;<sup>10</sup> the purpose of the current analysis is to test the effect of space collapse on fast breeder fuel-cycle parameters.

Specifically, the equations which describe a fuel-cycle analysis form a mildly nonlinear initial value problem. The reactor system and calculational model to which these equations are applied are described in detail in Ref. 11, and it is sufficient

for our purposes here to note that the system is a fast breeder with a mixed-oxide,  $UO_2$ - $PuO_2$  core ( $H/D = 0.16$ ) and  $UO_2$  blankets. The main computational difficulty in this problem is the approach to equilibrium because, during this time, the changes in the spatial and spectral distribution are greatest. In general, the changes involve an increase in the flux in the outer blankets, plus a hardening of the spectrum in these regions. The core distribution changes very little.

The technique is applied here in space collapsing the finite difference equations to perform the fuel-cycle analysis. The trial solution is taken as the fine-group (49), fine-spatial-mesh (1462) computation of the initial condition. In order to determine the effectiveness of this procedure, three fuel-cycle computations were performed through six burnup intervals and compared with the reference calculation. This reference computation utilized all 1462 spatial mesh points but was collapsed to eight energy groups. The test calculations also used the same eight energy groups, but with 49, 225, and 342 spatial mesh points for Cases 1, 2, and 3, respectively. In these latter calculations, the 225 and 342 mesh problems differ fundamentally from the 49-mesh calculation in that, in the 49-mesh case, both the cross sections and leakages were energy collapsed at each mesh point. In Cases 2 and 3, the cross-section data used is the same as that used in Case 1, but the leakage coefficients were collapsed for each of the mesh points. The effect of this approximation will be tested at a later date.

The effect of space collapsing on certain fuel-cycle parameters was examined at three time points: (1) beginning-of-life, (2) third burnup interval, and (3) equilibrium value, and for three regions--the core, the inner axial blanket, and the outer axial blanket. For each of the cases, the distribution of mesh points throughout the reactor is shown in Table 465-VI.

TABLE 465-VI  
 MESH POINT DISTRIBUTION

	Core	Blankets	Total
Reference	250	772	1462
Case 1	3	20	49
Case 2	9	145	225
Case 3	22	228	342

As seen from the table, the bulk of the mesh points added to those of Case 1 were added in the blankets. The reason is that the core flux distribution changes very little in time, while that of the blanket changes significantly, especially in the outer regions. The results of the calculations are shown in Table 465-VII. As can be seen from this data, mesh points do significantly improve the calculation. Also, it is seen that satisfactory fuel-cycle parameters may be obtained, even when the number of space points used is reduced by a factor of thirty as long as the data is collapsed correctly.

TABLE 465-VII

EFFECT OF A SPACE-COLLAPSED ANALYSIS  
OR SOME FUEL-CYCLE PARAMETERS

BREEDING RATIOS (% error)

Time	Reference	Case 1	Case 2	Case 3
1	1.1471	0.1	0.1	0.1
2	1.1883	-1.9	-1.4	-0.8
3	1.1852	-2.5	-1.7	-0.9

<sup>239</sup>Pu ATOM DENSITIES (% error)

a. Core

Time	Reference	Case 1	Case 2	Case 3
1	9125	0.0	0.0	0.0
2	8396	-0.2	-0.1	-0.1
3	8284	-0.3	-0.2	-0.2

b. Inner Axial Blanket

1	658	0.0	0.2	0.2
2	1465	-1.7	-1.3	-0.9
3	1693	-2.3	-1.8	-1.2

c. Outer Axial Blanket

1	318	0.0	0.0	0.0
2	745	-3.8	-2.4	-1.2
3	883	-5.1	-3.3	-1.6

REFERENCES

1. Donald J. Dudziak, "Translation to ENDF/B and 'Physics' Checking of Cross Sections for Shielding," DASA-2379 (ENDF-130), University of Virginia (1969).
2. M. K. Butler, Marianne Legan, and L. Ranzini, "Argonne Code Center: Compilation of Program Abstracts," ANL-7411, Argonne National Laboratory (1968).
3. R. W. Hardie and W. W. Little, Jr., "3DB, A Three-Dimensional Diffusion Theory Burnup Code," BNWL-1264, Battelle Northwest Laboratory (1970).
4. R. Douglas O'Dell and Thomas J. Hiron, "PHENIX, A Two-Dimensional Diffusion-Burnup-Refueling Code," LA-4231, Los Alamos Scientific Laboratory (1970).
5. R. Douglas O'Dell and Thomas J. Hiron, "PHENIX, A Two-Dimensional Diffusion-Burnup-Refueling Code," Nucl. Sci. and Eng. **39**, 411 (1970).
6. "Quarterly Status Report on the Advanced Plutonium Fuels Program, July 1 - September 30, 1969," LA-4307-MS, Los Alamos Scientific Laboratory (1969).
7. Private communication.
8. K. D. Lathrop, "DTF-IV, A FORTRAN-IV Program for Solving the Multigroup Transport Equation with Anisotropic Scattering," LA-3373, Los Alamos Scientific Laboratory (1965).
9. Private communication.
10. R. E. Alcouffe, T. J. Hiron, and R. D. O'Dell, "Spectral Effects on Calculated Fuel-Cycle Parameters in Large Fast Breeders," Trans. Am. Nucl. Soc. **12**, 695 (1969).
11. Thomas J. Hiron and R. Douglas O'Dell, "Calculational Models for Fast Reactor Fuel-Cycle Analysis," accepted for publication in Nucl. Appl. and Tech., will appear in July 1970 issue.

## PROJECT 467

### FUEL IRRADIATION EXPERIMENTS

Person in Charge: D. B. Hall  
Principal Investigator: J. C. Clifford

#### I. INTRODUCTION

The goal of this program is to examine the irradiation behavior of advanced fuels for LMFBRs. At present, the fuel concepts under study are sodium-bonded mixed carbides and metals. However, because of the decreasing interest in metals as LMFBR fuels, metal fuel work has been reduced and will be terminated by the end of the fiscal year.

Carbide investigations center around the irradiation performance of high purity, single-phase  $(U_{0.8}Pu_{0.2})C$  produced and characterized at the Los Alamos Scientific Laboratory (Project 463). Sodium-bonded, mixed-carbide pins are being irradiated in the EBR-II reactor at heat ratings of interest for fast reactor application. The experiments are designed to examine the degree of fuel swelling, gas release, fuel-sodium-clad interaction, and the migration of fissionable material and fission products as a function of burnup and fuel density. Thermal flux irradiations of LASL-produced carbides also are included to augment determination of the effects of high burnup on fuel-bond-clad compatibility.

#### II. EBR-II IRRADIATION TESTING

(J. O. Barner)

##### A. General

The purpose of the EBR-II irradiations is to evaluate candidate fuel/sodium/clad systems for the LMFBR program. In the reference design, fuel pellets of single-phase  $(U, Pu)C$  are separated by a sodium bond from a cladding of Type 316 stainless steel. Three series of

experiments are planned and approval-in-principle has been received from the AEC.

The capsules are to be irradiated under the following conditions:

Condition	Series 1	Series 2	Series 3
1. Lineal power, kW/ft	~ 30	~ 45	~ 30
2. Fuel composition	$(U_{0.8}Pu_{0.2})C$ , single-phase, sintered		
3. Fuel uranium	$^{235}U$	$^{233}U$	$^{235}U$
4. Fuel density	90%	95%	95%
5. Smear density	80%	80%	80%
6. Clad size	0.300-in. i.d. x 0.010-in. wall		
7. Clad type	316 SS	316 SS	316 SS
8. Max clad temp, °F	1250	1275	1250
9. Max fuel center-line temp, °F	2130	2550	2100
10. Burnup	3 a/o to 8 a/o		

The capsules are doubly contained.

##### B. Current Results

Two capsules from Series 1, designated K-42B and K-36B, currently are operating in EBR-II. They will be discharged from EBR-II for destructive examination about August 1, 1970, at burnups of 4.5 a/o and 3 a/o, respectively.

Three capsules from Series 1, designated K-37B, K-38B, and K-39B, and two capsules from Series 3, designated K-43 and K-44, have been shipped to EBR-II and are available for irradiation.

Preparation for the loading of the Series 2 capsules are complete except for fabrication of approximately 1/3

of the required fuel. These capsules will be loaded when acceptable fuel is fabricated.

The "data packages" for the Series 1 and 3 experiments have been completed and sent to EBR-II project personnel.

### III. THERMAL IRRADIATIONS OF SODIUM-BONDED MIXED CARBIDES (J. C. Clifford)

#### A. General

Mixed carbides, sodium-bonded to Type 316 stainless steel cladding are being irradiated in the LASL Omega West Reactor (OWR), a 6 MW MTR-type facility. The purpose of the experiments is to determine whether fuel, clad, and sodium remain mutually compatible as burnups of interest in the LMFBR program are approached. While fast-spectrum irradiations are preferred in order to produce the power densities and radial temperature gradients anticipated in LMFBRs, thermal irradiations appear acceptable in this instance because the fuel regions of prime interest (those in contact with sodium) for compatibility studies can be maintained at realistic temperatures.

Experiments are conducted in instrumented environmental cells installed semi-permanently in the OWR. The principal features of these cells are: (1) a heat removal and temperature control system consisting of a natural convection sodium loop, electrical heaters, and a variable conductivity heat leak, and (2) a sweep gas system for the rapid detection of leaking fuel capsules.

#### B. Current Results

Two environmental cells installed in the OWR core are being used for irradiation of sodium bonded, mixed carbides. One carbide experiment has been completed and two more are under way. The experiments are identical and each consists of two Type 316 stainless steel capsules, 2.5-in. long and 0.300-in. diam with 0.010-in. thick walls. Each capsule contains three pellets of 95% theoretical density, single-phase mixed carbide, a stainless steel insulator pellet to separate the fuel from the lower closure weld, and approximately 1/3 g Na. The uranium in the fuel is fully enriched in <sup>235</sup>U.

The capsules are stacked end on end at the axial center of a 0.600-in.-diam stainless steel secondary

container. The annular volume between capsules and secondary is filled with sodium, and capsules are centered in the secondary by thin stainless steel disks at the top and base of each capsule. An experiment contains eight thermocouples for monitoring temperatures of the fuel capsules and secondary sodium.

Measurements of fission heating in the three experiments indicate that each operates at a linear heat rating of approximately 22 kW/ft. Corresponding specific powers vary from approximately 650 W/g at the fuel surface to 170 W/g at the fuel centerline. Fuel surfaces are maintained in the range 600-700°C. Figure 467-1 shows the predicted radial temperature distribution based on a clad outside surface temperature of 640°C which is close to the maximum for each experiment. Figure 467-2 shows a predicted radical power distribution, neglecting end effects.

OWREX-14, the first carbide experiment, has completed a scheduled 55 day irradiation and has been removed for destructive examination. Predicted skin burnup for this experiment is 4 a/o. Irradiation of OWREX-15 was begun in January and will be terminated at 8 a/o skin burnup in June. OWREX-16 was inserted in the reactor in late March and is planned for operation to 10-12 a/o, requiring the remainder of the calendar year. At present, OWREX-15 and -16 are operating satisfactorily.

### IV. THERMAL IRRADIATION OF SODIUM-BONDED U-Pu-Zr (J. C. Clifford)

The program to evaluate the performance of LASL-produced U-Pu-Zr alloys through thermal irradiations and out-of-pile fuel/clad compatibility tests has been terminated except for the post-test examination of compatibility experiments in progress. Results from these experiments will be summarized in a topical report.

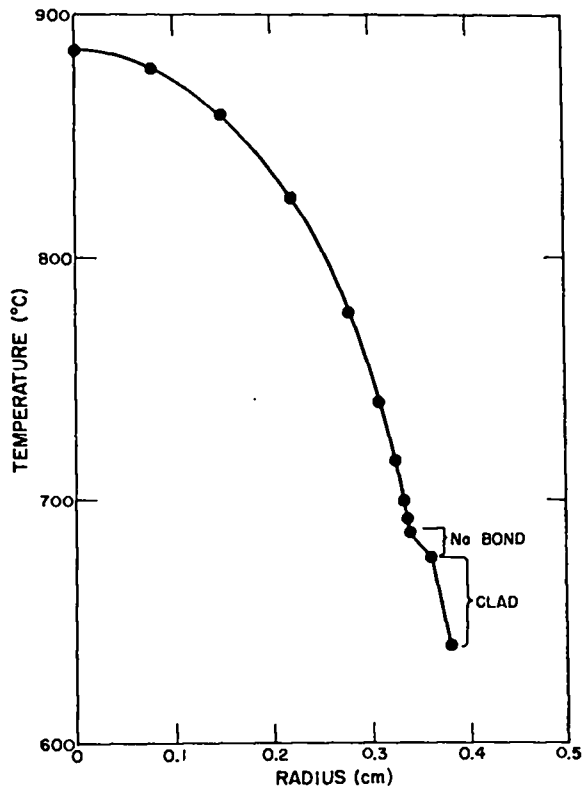


Fig. 467-1. Radial temperature distribution in OWREX-14 fuel capsule neglecting end effects.

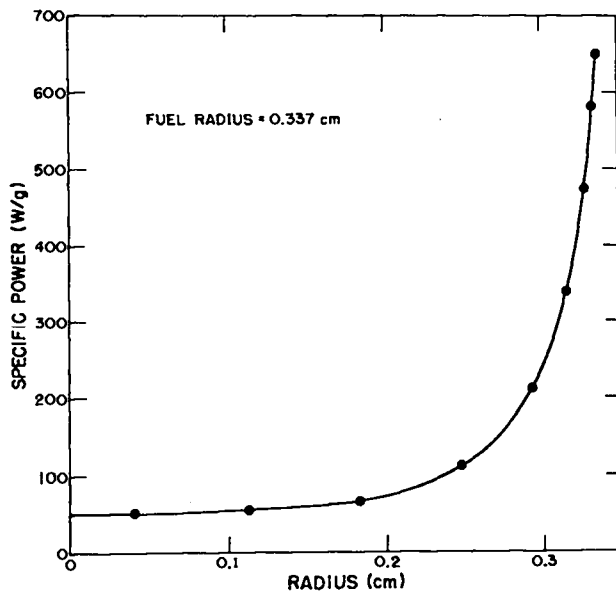


Fig. 467-2. Predicted radial power distribution in OWREX-14 fuel.

## PROJECT 501

### STANDARDS, QUALITY CONTROL, AND INSPECTION OF PRODUCTS

Person in Charge: R. D. Baker  
Principal Investigator: C. F. Metz

---

#### I. INTRODUCTION

A major factor in the development of a successful reactor fuel is a high degree of technical competence for doing the required chemical analysis and related measurements necessary to characterize thoroughly the raw materials, the manufactured fuel, and the irradiated fuel. This project is identified with the mixed oxide fuel development phase of the LMFBR/FFTF Program.

This project is directed toward (1) developing an analytical chemistry and measurements program, thereby ensuring high quality and uniformity of raw materials, (2) establishing and conducting a statistically designed quality control program of chemical analyses and other measurements that can be used to assure continuing adequate analytical competence of the fuel producers during the fuel fabrication stage, and (3) doing correlated chemical analyses and related measurements on irradiated fuel as a means of studying fuel behavior during core life; specifically involved will be burnup studies correlated with microprobe and metallography studies, gas release studies as related to cladding corrosion, and gas retention studies as related to porosity, particle size, and other properties of the fuel.

#### II. PHASE II, LMFBR/FFTF FUEL DEVELOPMENT ANALYTICAL CHEMISTRY PROGRAM

The remainder of the analytical data was received from participating laboratories, and all data were statistically examined. The results including evaluation of the methods used, the capabilities of each

participating laboratory and the analytical problems remaining to be solved, were published in LA Report No. 4407, entitled, "LMFBR/FFTF Fuel Development Analytical Chemistry Program, (Phase II)".

Bids for two mass spectrometers were received and evaluated, and purchase requests issued. One of these instruments will be used on burnup studies, and the other mainly on fission gas analyses with some work on gas retention problems. Standards were prepared for mass spectrometer calibrations.

Plans were completed and requests initiated for laboratory remodeling to house the mass spectrometers and in which to carry out burnup and gas retention studies.

#### III. INVESTIGATION OF METHODS

1. O/M Atom Ratios in Sintered (U, Pu)O<sub>2</sub>  
(G. C. Swanson, J. W. Dahlby and  
G. R. Waterbury)

Modifications to two thermogravimetric methods were made to improve the quantitative measurement of O/M atom ratio which is a chemical property having a significant effect on oxide fuel behavior. In the first of the modified methods, the change in weight of a 3- to 5-gram sample as it was oxidized in air and then reduced for 6 h at 1000°C in a 1 liter/min flow of He-6% H<sub>2</sub> was used to calculate the O/M atom ratio of the original oxide. These reduction conditions were established as a result of repeated tests on 3 : 1 mixtures of UO<sub>2</sub> and PuO<sub>2</sub> prepared with known oxygen contents from the pure metals (>99.99% pure). The

final oxide produced by these oxidation and reduction conditions was the stoichiometric dioxide as required in the assumptions made in calculating the O/M atom ratio. The standard deviation of the modified method was 0.002 and the bias in analyzing powders prepared from the two oxides was no larger than 0.002.

Investigation of this modified method was concluded by determining the effects on the O/M measurement of impurities that either are commonly found in sintered mixed oxide fuels or are included in the tentative FFTF fuel specifications. Portions of a  $(U_{0.75}Pu_{0.25})O_2$  powder made from the pure metals with known oxygen content were well mixed with the added impurities, and the O/M ratio was determined as described. It was found the 500 to 1300 ppm of Fe,  $Fe_2O_3$ , CaO, Ni, or  $Ni_2O_3$ , when added individually, did not affect the O/M by as much as 0.005, but similar amounts of C, Al,  $Al_2O_3$ , Ca, or  $Na_2SO_4$  caused errors as large as + 0.094 (Table 501-I). Six impurity elements (Al, Cr, Fe, Ni, Si, and Ti) included in the specifications did not affect the method when added collectively as oxides at metal concentrations ranging between 160 and 240 ppm, but similar amounts of the metals caused a large negative bias.

In the second modified method, the O/M ratio was calculated from the change in weight as a 3- to 5-gram sample was heated in Ar-8% containing 4 mm partial pressure of  $H_2O$ . Previous work showed that a

Table 501-I  
Effects of Selected Impurities on the Thermogravimetric Determination of O/M Ratio

Element	Form	Concentration, ppm <sup>a</sup>	Effect on O/M Ratio <sup>b</sup>
Fe	metal	967	-0.004
	$Fe_2O_3$	655	-0.001
Ni	metal	1,048	-0.012
	$Ni_2O_3$	625	-0.003
Ca	metal	1,000	-0.012
	CaO	799	-0.003
C	elemental	964	+0.013
Al	metal	997	-0.023
	$Al_2O_3$	536	-0.007
Na, S	$Na_2SO_4$	700	+0.094
Al, Cr, Fe, Ni, Si, Ti }	metal	160 to 240 mg each	-0.032
	oxides	140 to 280 mg each	-0.001

<sup>a</sup>ppm of the element whether added as metal, oxide, or compound.

<sup>b</sup>average of duplicate determinations.

reaction temperature greater than 1000°C was required to produce a stoichiometric dioxide, and further that this oxide had to be cooled in dry Ar-8%  $H_2$  to prevent weight increases due to moisture pickup. It was found that  $UO_{2.000}$  was produced by this method when  $U_3O_8$  was heated for 20 h at 1250°C (Table 501-II). For  $(U_{0.75}Pu_{0.25})O_2$  mixtures, essentially stoichiometric dioxides were produced in 16 h at 1250°C in this gas mixture.

Table 501-II  
O/M Ratios of Oxides Heated at 1250°C in Ar - 8%  
He - 4 mm  $H_2O$  Pressure

Oxide	Time at 1250°C, hr	No. of Determinations	Av. O/M <sup>a</sup> of Product
$U_3O_8$	7	4	2.004
	15	4	2.002
	20	4	2.000
(U, Pu) $O_2$	8	6	2.003
	16	5	2.002
	24	3	2.002

<sup>a</sup>Each oxide cooled in dry Ar - 8%  $H_2$  before weighing.

Plots of sample weight versus temperature obtained for 300 to 350-mg samples of  $U_3O_8$  using an automatic microthermogravimetric analyzer showed also that the O/M ratio was 2.002 following heating of the oxide in dry Ar-6%  $H_2$  at 1000°C until constant weight was attained. This required about 2 h. The O/M ratio of the oxide produced by heating in Ar-8%  $H_2$ -4 mm  $H_2O$  pressure at 1000°C was 2.017 which is in agreement with the value obtained with the macrothermogravimetric apparatus for 3- to 5-gram samples in this temperature range.

Based on these investigations, the modified method, in which the sample is oxidized in air and then reduced in dry He-6%  $H_2$  at 1000°C, was selected for further use. A final report is being prepared describing in some detail this development work and the modified method.

## 2. Gas Evolution from Sintered (U, Pu) $O_2$ (D. E. Vance, M. E. Smith, and G. R. Waterbury)

Measurements of the volumes of gases, including  $H_2O$  vapor, that are evolved from mixed oxide fuels at operating temperatures were required to estimate

increases in the internal pressures developed in sealed reactor fuel capsules. The  $H_2O$  released from sintered mixed-oxide pellets at  $800^\circ C$  was measured by sweeping the off-gas to a moisture monitor and integrating the monitor signal. To determine if  $800^\circ C$  was adequate to evolve the  $H_2O$  quantitatively, pellets that had been heated to  $800^\circ C$  were reheated to  $950^\circ C$ . Additional gas was not collected at the higher temperature.

Gases other than  $H_2O$  were evolved by heating the sintered mixed-oxide inductively in a W crucible to  $1600^\circ C$ . These gases were dried over anhydrous  $Mg(ClO_4)_2$  and measured manometrically. A decrease in the apparatus blank and an improvement in the reliability of the method were obtained by installing a new type of induction furnace and an all-stainless-steel manifold in the apparatus.

Some preliminary data were obtained on the volumes and compositions of the gases collected at various temperatures. Outgassing of  $(U, Pu)O_2$  sintered oxide was almost complete (>98%) at  $1300^\circ C$ , but a very small volume of gas was collected at  $1900^\circ C$ . The major constituent of these gases was  $H_2$ . At  $2100^\circ C$ , a large fraction of the sample vaporized and coated the inside of the furnace tube. Differences in the apparatus blanks at the various temperatures caused some difficulties in interpreting the data, and methods for eliminating or compensating for these differences are being investigated before further determinations are made.

### 3. Spectrochemical Analysis of $PuO_2$ Raw Material (W. M. Myers and R. T. Phelps)

The chemical purity of the  $UO_2$  and  $PuO_2$  raw materials is one determining factor in control of the quality of the sintered  $(U, Pu)O_2$  product, and reliable measurement of spectrographic impurities is required. Previously reported methods apply to most spectrographic impurities in the starting oxides, but are insensitive to Ta and Zr at concentrations below 2000 ppm in  $PuO_2$ .

A carrier distillation method that uses AgCl as the carrier was modified to improve the sensitivity for measuring Ta and Zr. Low-background, type SA-1, photographic emulsion plates were substituted for the faster 103-0 type plates to aid in the photometric

measurement of the Zr lines, and Pd was used as an internal standard. Under these conditions, Ta and Zr were measured in the concentration range between 50 and 1000 ppm with a standard deviation of 20 relative percent.

### 4. Measurement of $N_2$ in $(U, Pu)O_2$ (G. C. Swanson and G. R. Waterbury)

Measurement of  $N_2$  at low concentrations in  $(U, Pu)O_2$  is necessary to ensure that the maximum concentration included in the specifications for FFTF fuel is not exceeded. A LECO Nitrox-6 analyzer was modified for this measurement by adding equipment to remove CO formed from  $O_2$  in the sample during the analysis. The  $N_2$ , evolved by heating the sample in a C crucible at  $2200^\circ C$ , is measured in a simple gas chromatograph following the separation from CO. Essentially complete recovery of the  $N_2$  from  $UO_2$  samples required about 45 min, and the apparatus blank for this long heating period was inordinately high. Additional purification of the He sweep gas, and brazing all joints in the gas analysis system reduced the 45-min blank to approximately  $50 \mu g$  of  $N_2$ . This blank is reproducible within  $\pm 1 \mu g$ , but a smaller blank would be advantageous. For this reason the furnace power supply of the apparatus was modified to increase the maximum crucible temperature to  $2350^\circ C$ . Tests are in progress to determine if a shorter analysis time, and therefore a smaller apparatus blank, is possible at the higher temperature.

SPECIAL DISTRIBUTION

Atomic Energy Commission, Washington

Division of Research

D. K. Stevens

Division of Naval Reactors

R. H. Steele

Division of Reactor Development and Technology

G. W. Cunningham

D. E. Erb

Nicholas Grossman

W. H. Hannum (2)

K. E. Horton

J. R. Humphreys

R. E. Pahler

J. M. Simmons (2)

E. E. Sinclair

Bernard Singer

C. E. Weber

G. W. Wensch

M. J. Whitman

Division of Space Nuclear Systems

G. K. Dicker

F. C. Schwenk

Safeguards & Materials Management

J. M. Williams

Idaho Operations Office

DeWitt Moss

Ames Laboratory, ISU

O. N. Carlson

W. L. Larsen

M. Smutz

Argonne National Laboratory

A. Amorosi

R. Avery

F. G. Foote

Sherman Greenberg

J. H. Kittel

W. B. Loewenstein

P. G. Shewmon

Idaho Falls, Idaho

D. W. Cissel

Milton Levenson

R. C. Robertson

Atomics International

R. W. Dickinson, Director (2)

Liquid Metals Information Center

J. L. Ballif

Babcock & Wilcox

C. Baroch

J. H. MacMillan

Donald W. Douglas Laboratories

R. W. Andelin

General Electric Co., Cincinnati, Ohio

V. P. Calkins

General Electric Co., Sunnyvale, California

R. E. Skavdahl

Gulf General Atomic, Inc.

E. C. Creutz

Idaho Nuclear Corporation

W. C. Francis

IIT Research Institute

R. Van Tyne

Lawrence Radiation Laboratory

Leo Brewer

J. S. Kane

A. J. Rothman

LMFBR Program Office

D. K. Butler (Physics)

P. F. Gast

L. R. Kelman (Fuel & Materials)

J. M. McKee (Sodium Technology)

Mound Laboratory

R. G. Grove

NASA, Lewis Research Center

J. J. Lombardo

Naval Research Laboratory

L. E. Steele

Oak Ridge National Laboratory

G. M. Adamson

J. E. Cunningham

J. H. Frye, Jr.

C. J. McHargue

P. Patriarca

O. Sisman

M. S. Wechsler

J. R. Weir

Pacific Northwest Laboratory

F. W. Albaugh

E. A. Evans

V. J. Rutkauskas

W. R. Wykoff

FFTF Project

E. R. Astley

B. M. Johnson

D. W. Shannon (2)

Battelle Memorial Institute

D. L. Keller  
S. J. Paprocki

Brookhaven National Laboratory

D. H. Gurinsky  
C. Klamut

Combustion Engineering, Inc.

S. Christopher

U. S. Department of Interior

Bureau of Mines, Albany, Oregon

H. Kato

United Nuclear Corporation

A. Strasser

Westinghouse, Advanced Research Division

E. C. Bishop

Australian Atomic Energy Commission

J. L. Symonds